GHENT UNIVERSITY
FACULTY OF PHARMACEUTICAL SCIENCES

Department of Pharmaceutics

Laboratory for Pharmaceutical technology

Academic year 2014-2015

EVALUATION OF FATTY ACIDS AS POTENTIAL MATRIX FORMERS FOR CONTROLLED RELEASE – A COMPARISON BETWEEN EXTRUSION AND PRILLING

Apr. Cathérine DEVIAENE

Master of Science in Industrial Pharmacy

Promoter
Prof. Dr. J.P. Remon

Commissioners
Prof. Dr. J.P. Remon

Prof. Dr. R. Kemel

Prof. Dr. G. Van den Mooter

Prof. Dr. T. De Beer

Dr. F. Kiekens

GHENT UNIVERSITY
FACULTY OF PHARMACEUTICAL SCIENCES

Department of Pharmaceutics

Laboratory for Pharmaceutical technology

Academic year 2014-2015

EVALUATION OF FATTY ACIDS AS POTENTIAL MATRIX FORMERS FOR CONTROLLED RELEASE – A COMPARISON BETWEEN EXTRUSION AND PRILLING

Apr. Cathérine DEVIAENE

Master of Science in Industrial Pharmacy

Promoter
Prof. Dr. J.P. Remon

Commissioners
Prof. Dr. J.P. Remon

Prof. Dr. R. Kemel

Prof. Dr. G. Van den Mooter

Prof. Dr. T. De Beer

Dr. F. Kiekens

COPYRIGHT

January 14, 2015

Promoter	Author
Prof. Dr. J.P. Remon	Cathérine Deviaene

SUMMARY

The aim of this study is the development and characterization of multiparticulate dosage forms which release MPT, a β-blocker, at a controlled rate. In order to achieve this goal, a solid dispersion is made by embedding MPT in a fatty acid matrix (behenic acid and myristic acid) via extrusion and prilling. The release out of the matrix is diffusion-based. Since controlled release dosage forms allow a lower dosing frequency and exhibit less side effects compared to immediate release dosage forms, patient compliance is improved.

Controlled release formulations were successfully produced via extrusion and prilling by adding a certain percentage of myristic acid to the behenic acid matrix. The release rate of the 30:70 MPT:BA extrudates was significantly faster compared to the 30:20:50 MPT:MA:BA extrudates and prills. As myristic acid is less hydrophobic than behenic acid, these results were not expected. The difference could be explained by molecular interactions between the fatty acids and/or between MPT and the fatty acids.

The solid state behaviour was characterized using Raman spectroscopy, modulated differential scanning calorimetry and X-ray diffraction. FT-IR spectroscopy was performed in order to identify intermolecular interactions. The results suggested that more interactions occurred during extrusion compared to prilling, which could be explained by more intense mixing by the screws.

As aging of lipids can occur during storage, the stability of the formulations was investigated during storage at 25 °C and 40 °C. The drug release rate from 30:20:50 MPT:MA:BA extrudates was significantly decreased after 1 month and 3 months storage at 40 °C compared to immediately after processing. The reason for this phenomenon is still unclear, as Raman and FT-IR spectroscopy, MDSC and XRD revealed no changes during storage.

The Raman spectra of the 30:20:50 MPT:MA:BA prills immediately after manufacturing indicated a decrease in crystallinity of myristic acid compared to the physical mixture and the presence of amorphous MPT. However, during storage at 25 °C and 40 °C, the peaks had sharpened again, indicating recrystallization.

SAMENVATTING

Het doel van deze studie is de ontwikkeling en karakterisatie van multiparticulaire doseervormen die metoprololtartraat (MPT), een β-blokker, op gecontroleerde wijze vrijgeven. Om dit doel te bereiken, wordt een solid dispersion aangemaakt door MPT in te bedden in een vetzuurmatrix (beheenzuur en/of myristinezuur) via extrusie en prilling. Doseervormen met gecontroleerde vrijgave laten een lagere doseringsfrequentie toe en veroorzaken minder nevenwerkingen in vergelijking met doseervormen met onmiddellijke vrijstelling. Hierdoor verbetert de therapietrouw.

Doseervormen met gecontroleerde vrijgave werden succesvol aangemaakt via extrusie en prilling door een bepaald percentage myristinezuur toe te voegen aan de beheenzuurmatrix. De in vitro vrijstellingssnelheid van de 30:70 MPT:BA extrudaten was significant sneller in vergelijking met de 30:20:50 MPT:MA:BA extrudaten en prills. Deze resultaten waren onverwacht aangezien myristinezuur minder hydrofoob is dan beheenzuur. Een mogelijke verklaring voor de tragere vrijstellingssnelheid na toevoeging van myristinezuur zijn interacties tussen de vetzuren en/of tussen MPT en de vetzuren.

De invloed van extrusie en prilling op de kristalliniteit van MPT en de vetzuren werd bepaald met behulp van Raman en FT-IR spectroscopie, gemoduleerde differentiaal scanning calorimetrie en X-straal diffractie. Uit de resultaten bleek dat extrusie meer intermoleculaire interacties veroorzaakte dan prilling. Een mogelijke verklaring voor dit fenomeen is een intensere menging tijdens extrusie veroorzaakt door de schroeven.

Aangezien lipiden wijzigingen in kristalliniteit kunnen vertonen tijdens bewaring, werd de stabiliteit van de formulaties tijdens bewaring bij 25 °C en 40 °C nagegaan. De vrijstellingssnelheid van MPT uit de 30:20:50 MPT:MA:BA extrudaten was significant gedaald na 1 maand en 3 maanden bewaring bij 40 °C in vergelijking met de vers aangemaakte formulatie. De oorzaak van dit fenomeen is nog onduidelijk. De Raman spectra van de verse 30:20:50 MPT:MA:BA prills toonden piekverbreding, wat wees op de aanwezigheid van een amorfe MPT fractie en een gedaalde kristalliniteit van myristinezuur ten gevolge van prilling. Tijdens bewaring trad er herkristallisatie op van beide componenten.

DANKWOORD

Een thesis schrijf je niet alleen. Veel mensen hebben een belangrijke rol gespeeld in het tot stand komen van deze masterproef. In dit dankwoord wil ik hen van harte bedanken voor hun hulp, steun en vertrouwen.

Eerst en vooral wil ik mijn promotor, Prof. Dr. J. P. Remon en Prof. Dr. C. Vervaet bedanken om mij de kans te geven om mijn masterproef in het labo voor Farmaceutische Technologie uit te voeren.

Mijn bijzondere dank gaat uit naar Apr. Anouk Vervaeck, voor de uitstekende begeleiding. Een welgemeend dankjewel voor de aangename samenwerking, het nalezen en verbeteren van mijn masterproef en het beantwoorden van talloze vragen.

Ik wil ook de andere doctoraatsstudenten bedanken voor hun hulp bij kleine problemen. Mijn collegae-thesisstudenten wil ik graag bedanken voor de aangename sfeer, voor hun luisterend oor en voor de fijne gesprekken.

Tenslotte bedank ik mijn ouders voor hun onvoorwaardelijke steun en vertrouwen.

TABLE OF CONTENTS

LIST OF ABBREVIATIONS

API:	Active pharmaceutical ingredient
BA:	Behenic acid
FT-IR:	Fourier-Transform Infrared
HME:	Hot melt extrusion
MA:	Myristic acid
MDSC:	Modulated differential scanning calorimetry
MPT:	Metoprolol tartrate
SEM:	Scanning electron microscopy
XRD:	X-ray diffraction

1 INTRODUCTION

1.1 EXTRUSION

1.1.1 Introduction

Extrusion can be defined as "*pumping raw materials with a rotating screw under elevated temperature through a die into a product of uniform shape*"(1). Hot melt extrusion (HME) has been widely used for decades in the plastics and rubber industry to manufacture pipes, hoses, sheets… The last years, HME has found its way to the pharmaceutical industry, under the form of granules, pellets, tablets (e.g. Norvir®, Kaletra®), vaginal rings (e.g. NuvaRing®, Implanon®), transdermal systems, ophthalmic inserts… (1-3)

HME is a promising continuous technique because of the possibility to obtain controlled release formulations (2, 4-6) and to mask the taste of the active pharmaceutical ingredient (API) (7-9). It can also be used to make a solid dispersion of the drug in the carrier in order to improve the release rate and the bioavailability of the API. A controlled release dosage form of an API with a good solubility can be produced by embedding the drug in a water insoluble matrix (2, 3, 10).

1.1.2 Technique

A schematic overview of a hot melt extruder is illustrated in Fig. 1.1. In a first step, the API and carrier have to be mixed to obtain a homogeneous powder blend. Secondly, the powder mixture is fed into the barrel. The screws in the barrel transport the powder mixture towards the die.

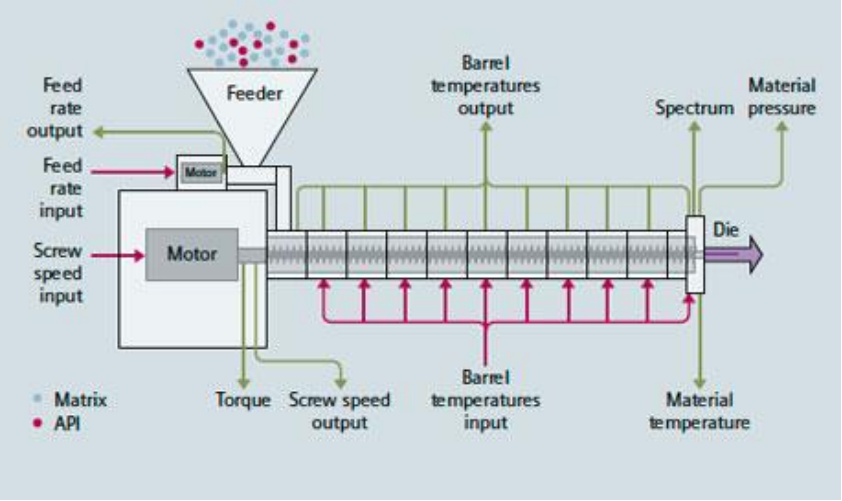

Figure 1.1: Schematic overview of a hot melt extruder (11).

The barrel of the extruder can consist of different zones, with the possibility of heating each zone to a different temperature. Inside the barrel of a twin screw extruder, the two screws co- or counter-rotate. A screw can consist of kneading elements and conveyer elements (Fig. 1.2). During transportation, the material is heated and kneaded, resulting in compression, melting and mixing of the mass. The mass is forced through the die, which determines the shape of the extrudate. Finally, the extrudates can be spheronized to produce spherical pellets by rotating them on a plate with grooves (1, 12, 13).

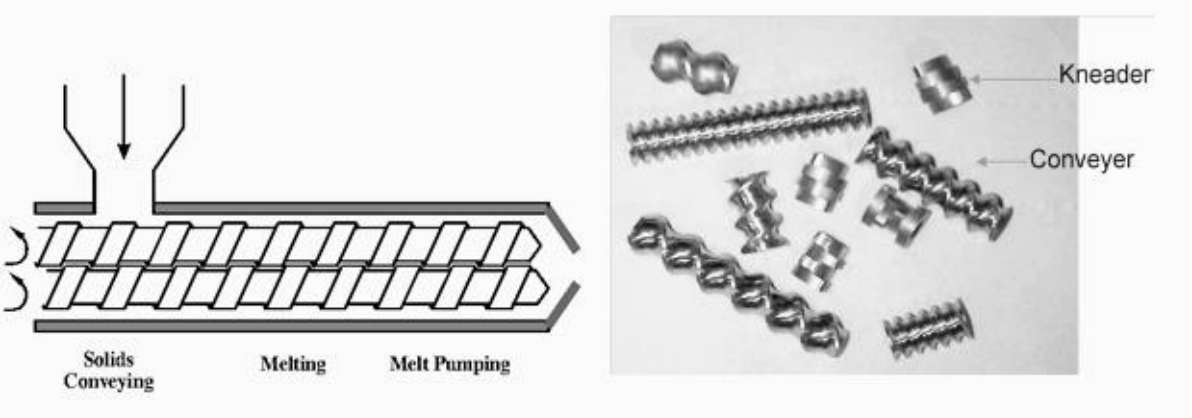

Figure 1.2: Cross-section of a twin screw extruder barrel (left) – Kneading and conveyer elements (right) (13).

1.1.3 Advantages and disadvantages

Since HME is an anhydrous technique, material degradation by hydrolysis is limited (1). No solvents are involved, which makes HME an environmentally friendly technique and which reduces the number of processing steps (1, 13). Mixing, melting and generating the solid dispersion all occur during one process (10). In-line measurements are possible, e.g. in-line characterization of the solid state and determination of the drug concentration using Raman spectroscopy (14-16).

As HME is often performed at high temperatures, the processed drugs and carriers have to be thermally stable. However, thermal degradation of the API or the carrier can be minimized by extruding at temperatures as low as possible. Other disadvantages are the need for excellent flow properties of the mixture and a high energy input (1).

In this study, a twin screw extruder is used for HME. Twin screw extrusion has several advantages over single screw extrusion. In twin screw extrusion, the residence time of the powder mixture is mostly no more than two minutes, so degradation of thermolabile substances is limited. Another advantage is a better mixing of the compounds by generating two types of mixing: distributive and dispersive mixing. Dispersive mixing results in size reduction, while distributive mixing generates a homogeneous mixture (10, 13, 17).

1.2 PRILLING

1.2.1 Introduction

Prilling or laminar jet breakup is a form of microencapsulation: a vibrating nozzle breaks up a laminar stream into small droplets, the drops fall down in a cold airstream, causing them to cool and solidify (18-20). Prilling has been widely used for the production of fertilizers such as ammonium nitrate and urea (19). More recently, the technique has been investigated as a method to produce immediate and controlled release multiparticulate dosage forms (18, 21, 22). An example of a commercial formulation prepared via prilling is Micropakine® (23).

1.2.2 Technique

The prilling process starts with the melting of the lipid components. Next, the API is dissolved or dispersed in the melt. The molten mixture is forced through vibrating calibrated nozzles, causing the flow to break up into droplets. These droplets fall down in a temperature-controlled prilling tower, where they are cooled and crystallized (20).

1.2.3 Advantages and disadvantages

Prilling is a continuous technique, which produces spherical particles (called prills) with a narrow particle size distribution. The obtained prills exhibit excellent flow properties, which allows capsule filling. Similar to extrusion is prilling an environmentally friendly technique because no solvents have to be used (20, 22, 24, 25).

During the process, the API and carrier are exposed to high temperatures, which limits the processing of thermolabile APIs. The major problem of prilling is the need of a tower which is high enough to solidify the droplets. This increases the cost of the process and makes operation and maintenance more difficult. The droplets have to be completely cooled when

they reach the bottom of the prilling tower to ensure that the particles do not aggregate. Solidification of the droplets starts at the surface and progresses towards the middle. The bigger the diameter of the droplets, the higher the prilling tower has to be in order to solidify the droplets before they reach the bottom of the tower. This limits the maximum diameter of the prills to 2 mm (19, 20, 22).

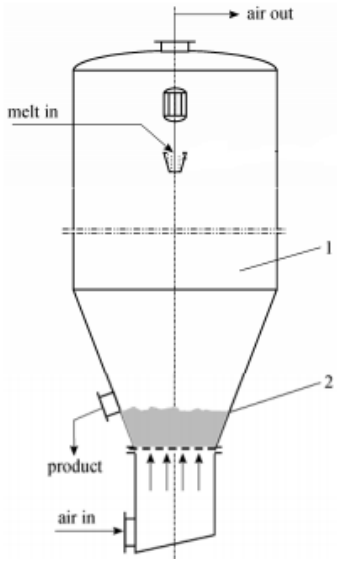

Figure 1.3: Combination of a prilling tower (1) with a fluidized bed (2) (19).

As shown in Fig. 1.3, a fluidized bed can be coupled to the prilling column. The fluidized bed increases the residence time of the droplets. Once the outer shell of the droplet is solidified in the tower, further solidification towards the middle can occur in the fluidized bed. By consequence, a shorter column can be used (19).

1.3 LIPIDS FOR ORAL DOSAGE FORMS

Lipids include waxes, fatty acids, triglycerides, oils… (26). Solid lipids exhibit several advantages: they have a low toxicity, they are biodegradable and they are low-cost (27). Lipid matrices can be used to create both immediate (21, 28, 29) and controlled release (5, 21, 22, 28, 30-32) formulations, to mask a bitter taste of the API (9, 28, 33), to improve the bioavailability of drugs with a low solubility (28, 34) and to generate floating drug delivery systems (27, 35).

The main disadvantage of lipids is the risk of degradation and aging during storage. Usually lipids exist in three polymorphic forms: the least stable α-form, the metastable β'-form and the stable β-form (27, 36, 37). Changes in polymorphism can affect the stability and the release characteristics of the formulation (26, 27).

Extrusion can be used to make lipid-based controlled release dosage forms. The temperature during the extrusion process and the friction generated by the screws have an effect on the polymorphic behaviour of the lipid carrier (36, 37). In solid lipid extrusion, the API and carrier are extruded at temperatures below the melting range of the lipids in order to avoid complete melting of the carrier (10). A study of Windbergs et al. showed that when extruding triglycerides, the temperature of the die needed to be higher than the melting point of the α-form of the triglyceride. Understanding the solid state behaviour during processing and storage is essential to produce stable formulations via extrusion (37). A change in drug release during storage has been observed in several studies (22, 31, 38).

Drug release out of the lipid matrix is diffusion-based. If the drug concentration is too low, only a part of the drug will be reached by the gastric fluid, resulting in incomplete release. When making a lipid-based formulation via prilling, it is important to determine the threshold below which the drug won't be completely released out of the matrix (30). On the other hand, if the drug concentration is too high, the viscosity of the mixture rises. This may lead to obstruction of the nozzle or the production of particles with a too large diameter (26).

Other techniques to produce oral solid lipid dosage forms are direct compression, dry and wet granulation, melt granulation, molding, spray congealing and hot melt coating. Direct compression is a simple continuous technique, but not all formulations can be processed via this method. When direct compression gives insufficient results, wet or dry granulation may be a good alternative. Being less used, molding is an easy method to produce lipid-based controlled release dosage forms. Molding includes dispersing of the API in molten lipids and filling this mixture into a mold (26).

1.4 CONTROLLED RELEASE

Two types of oral dosage forms are possible: immediate release and controlled release dosage forms. Fig. 1.4 shows the difference between single and multiple doses of a conventional dosage form. Also the difference between sustained and zero-order controlled release is illustrated.

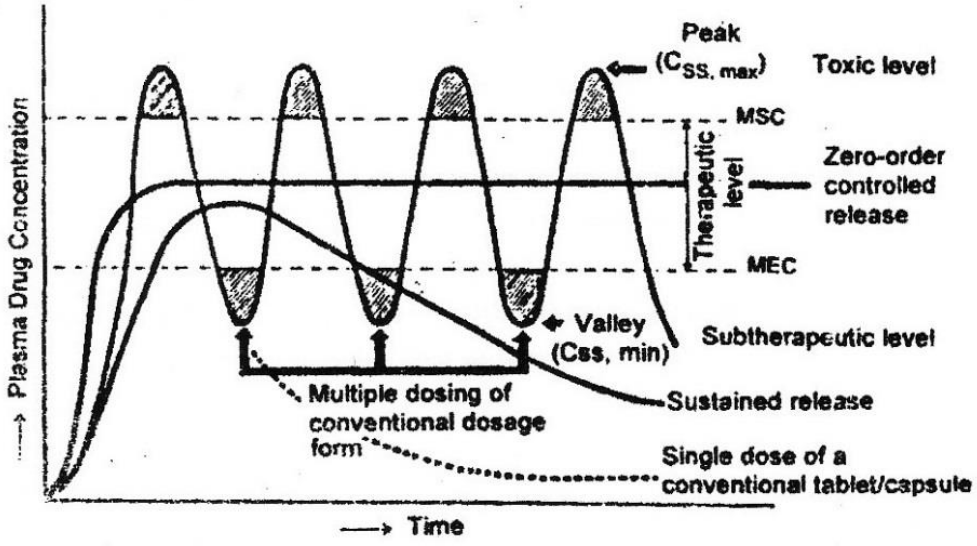

Figure 1.4: Immediate and controlled release dosage forms (39).

When an immediate release dosage form is administered, the plasma drug concentration increases very fast. However, the concentration decreases very quickly to subtherapeutic levels. This results in the need for frequent administration of drugs with short half-life, which may lead to bad patient compliance. When multiple doses of a conventional dosage form are administered, it is possible that the plasma drug concentration reaches toxic levels (39, 40). This might be dangerous when using drugs with a narrow therapeutic range, e.g. aminoglycosides, vitamin K antagonists, digoxin, lithium, theophylline… (41)

Controlled release formulations release the drug at a controlled rate during an extended period of time. Therapeutic concentrations are reached for a longer period compared to immediate release formulations, which makes reduction of the dose and the dosing frequency possible. Controlled release formulations yield less side effects, therefore enhancing patient compliance. Disadvantages of controlled release systems are the risk of dose dumping, more difficult dose adjustments and higher manufacturing costs (39, 40).

The release mechanism out of controlled release oral dosage forms can be based on dissolution/erosion, diffusion, osmosis and ion exchange. Dosage forms based on dissolution or diffusion can be divided into two categories, a matrix system and a reservoir system. In a matrix system based on diffusion, the API is homogeneously dispersed in a water insoluble carrier. Water flows into the matrix, the API dissolves and diffuses out of the matrix. A reservoir based on diffusion consists of an insoluble but permeable membrane around the API-containing core. The API diffuses through this membrane towards the external environment. A tablet coated with a water-soluble coating forms a reservoir system based on dissolution. In a matrix system based on dissolution, the API is dispersed in a water-soluble carrier. An osmotic-controlled release dosage form consists of a core containing the API and a surrounding semipermeable membrane. Via the semipermeable membrane, water flows into the system and the pressure rises. Consequently, the API is released via an orifice at a constant rate (42).

1.5 SOLID DISPERSIONS

A solid dispersion can be defined as *"a dispersion of one or more active ingredients in an inert carrier at the solid state, prepared by the melting, the solvent or the melting-solvent method"* (43). Some commercially available solid dispersions are Cesamet®, Kaletra®, Sporanox®, Certican®, Nivadil® and Prograf® (43).

Solid dispersions can be used to produce controlled release dosage forms and they have proven to be a good strategy to enhance the bioavailability of poorly soluble drugs (3, 40, 44). They represent a smaller particle size, an improved wettability and a higher porosity, resulting in a higher release rate and an improvement of the bioavailability (45). However, the development of solid dispersions can encounter problems: when a large amount of carrier is necessary to produce a solid dispersion, the dosage form may become too large to be easily swallowed.

Solid dispersions include eutectic mixtures, solid solutions and glass solutions and suspensions. Eutectic mixtures consist of two compounds that are completely miscible in the liquid state, but not in solid state. When the compounds are in the eutectic composition, they will crystallize at the same temperature and only one melting peak will be visible in a DSC

thermogram. In other compositions, one of the components crystallizes before the other during cooling. Solid solutions consist of one phase: the API (solid solute) and the matrix components (solid solvent) are miscible in both the liquid and the solid state. In solid solutions, the API is molecularly dispersed in a crystalline matrix. Only one melting peak will be observed in the thermogram. In glass solutions and glass suspensions, the carrier is in the amorphous state. In a glass solution, the API is molecularly dispersed in the amorphous carrier. Only one glass transition will be observed in a DSC thermogram. In a glass suspension, the API can be in a crystalline state or in an amorphous state. When both the API and the carrier are in the amorphous state, two glass transitions will be observed in a DSC thermogram, when the API is in a crystalline state and the carrier in an amorphous state, a glass transition and a melting peak will be present (43-46).

Solid dispersions are generally prepared by the fusion method or the solvent evaporation method. The fusion method consists of melting the API and the carrier, after which the mixture is cooled and pulverized. The fusion method is a relatively simple and low-cost method. Disadvantages of this method are the formation of an inhomogeneous solid dispersion when the API and the carrier are incompatible and the fact that the carrier and the API have to be stable at the process temperature (44-47).

The solvent evaporation method starts with dissolving both the carrier and the API in a common solvent. Then, the solid dispersion is formed by evaporating the solvent at low temperature. In contrast to the fusion method, the solvent evaporation method is suitable for thermolabile drugs. On the other hand, the use of solvents is cost- and time-consuming. Moreover it is a challenge to find a solvent in which both API and carrier are soluble (44-47).

1.6 CONTROLLED RELEASE MULTIPARTICULATE DOSAGE FORMS

The aim of this study is to develop controlled release multiparticulate dosage forms. A multiparticulate dosage form can be defined as *"a system that consists of multiple mini drug depots wherein the drug is either dispersed in a matrix or encapsulated in a reservoir"* (24). These mini drug depots (pellets, granules, mini tablets, micro- and nanoparticles) can be compressed into a tablet or can be easily filled into a capsule because of their ideal flow properties (21, 24).

Controlled release multiparticulate dosage forms have several advantages over single unit dosage forms. After oral intake, the tablet or capsule disintegrates in the stomach and the API is released from the individual mini drug depots. There are less gastro-intestinal side effects compared to single unit dosage forms, there is no risk of dose dumping and the absorption and bioavailability are increased. The dosing frequency is lower compared to single unit dosage forms, resulting in a higher patient compliance. Lower intra and inter subject variability in bioavailability and drug plasma concentrations is another advantage (4, 24, 48). Disadvantages of controlled release multiparticulate dosage forms include higher manufacturing cost, lower drug loading and more complicated production processes (49).

Multiparticulate dosage forms can be used to reduce the variability in gastric retention time, therefore reducing variability in bioavailability (49, 50). Other applications are the co-administration of incompatible drugs, the combination of pellets with different release rates (24) or the creation of pulsatile drug delivery (49).

2 OBJECTIVES

The aim of this study is to produce controlled release formulations of metoprolol tartrate (MPT), a hydrophilic drug, via both extrusion and prilling. MPT is a cardioselective β-blocker used for the treatment of hypertension and several other cardiovascular conditions. Since controlled release dosage forms allow a lower dosing frequency and exhibit less side effects compared to immediate release dosage forms, patient compliance is improved. Myristic acid and/or behenic acid are used to create a lipid matrix, which releases MPT via diffusion.

The temperature of the extruder and the friction caused by the screws determine the solid state of the extrudate. As prilling is performed at 100 °C and the droplets are finally quench cooled, the solid state may be influenced by the extreme process conditions. Therefore, the solid state of the formulations has to be examined. Extrudates and prills with same composition will be processed via both techniques in order to compare their solid state.

The solid state behaviour is characterized using Raman spectroscopy, MDSC and X-ray diffraction. FT-IR spectroscopy is performed in order to identify molecular interactions. The surface of extrudates and prills is visualized using scanning electron microscopy.

As aging of lipids can occur during storage, changes in crystallinity during storage have to be examined as well. Changes in solid state may influence the in vitro drug release. Therefore, the formulations are filled in hermetically sealed bags and stored in ovens of 25 °C and 40 °C to determine the stability of the formulations during storage. In vitro drug release testing, Raman and FT-IR spectroscopy and MDSC are performed after 1 week, 1 month and 3 months storage. After 3 months, the formulations are evaluated using XRD as well.

3 MATERIALS AND METHODS

3.1 MATERIALS

3.1.1 Metoprolol tartrate

Metoprolol tartrate (MPT) (Esteve Quimica, Barcelona, Spain) is a cardioselective β-blocker, which is used for the treatment of hypertension, angina pectoris, secondary prevention after myocardial infarction and stable chronical heart failure. Examples of commercial formulations containing MPT are Lopresor® and Seloken® (51). MPT has a molecular weight of 684.82 g/mol and a melting point of 120 °C (52, 53). It is highly soluble in water and it has a high permeability (52, 54).

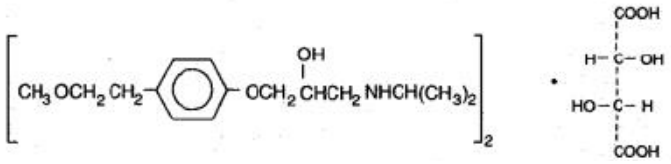

Figure 3.1: Structural formula of metoprolol tartrate (55).

3.1.2 Behenic acid

Behenic acid (BA, $C_{22}H_{44}O_2$) (Oleon, Ertvelde, Belgium) is a saturated fatty acid with a molecular weight of 340.59 g/mol. It is insoluble in water and has a melting point of approximately 80 °C. Behenic acid is found in large amounts in jamba oil, mustard seed oil and rape oil (52, 56).

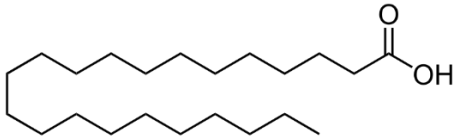

Figure 3.2: Structural formula of behenic acid (57).

3.1.3 Myristic acid

Myristic acid (MA, $C_{14}H_{28}O_2$) (Mosselman, Ghlin, Belgium) is a saturated fatty acid with a molecular weight of 228.38 g/mol. It can be found in most animal and vegetable fats. It is found in large amounts in nutmeg butter. Myristic acid is insoluble in water and has a melting point of 53.9 °C (52, 58).

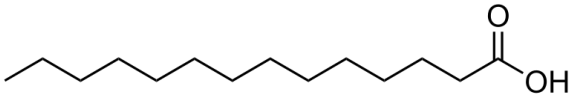

Figure 3.3: Structural formula of myristic acid (59).

3.2 METHODS

3.2.1 Extrusion

The extrusion process was performed using a co-rotating twin screw extruder (Prism Eurolab 16 TSE, Thermo Fischer Scientific, Karlsruhe, Germany). After weighing, the powder mixtures were blended for 15 min with a Turbula Mixer (Willy A. Bachofen AG Maschinenfabrik, Muttenz, Switzerland). These mixtures were then transferred to a gravimetric powder feeder (DD Flexwall® 18 feeder (Brabender Technologie, Germany)) which feeds the powder to the barrel of the extruder. The barrel consists of 6 segments. The temperature of the die and the different segments could be controlled separately. All mixtures were extruded using a screw speed of 40 rpm and a throughput of 0.3 kg/h, except pure behenic acid, which was extruded with a throughput of 0.4 kg/h. The composition and extrusion parameters of the different mixtures is presented in Table 3.1. After extrusion, the extrudates containing MPT were manually cut into mini-cylinders with a length of 4 mm ± 0.3 mm.

Table 3.1: Composition and extrusion parameters of the different mixtures.

MPT (%)	MA (%)	BA (%)	Die (°C)	Z6 (°C)	Z5 (°C)	Z4 (°C)	Z3 (°C)	Z2 (°C)	Torque (%)
		100	70	70	70	70	70	70	58-65
		100	75	80	80	80	80	80	22-30
	100		45	45	45	45	45	45	26-31
	100		45	55	60	60	60	60	16-19
	28.57	71.43	50	50	50	50	50	50	12-15
	28.57	71.43	50	60	60	60	60	60	8-11
	28.57	71.43	45	60	80	80	80	80	2-3
	50	50	45	45	45	45	45	45	15-18
	50	50	40	50	60	60	60	60	4-6
	71.43	28.57	45	45	45	45	45	45	12-18
	71.43	28.57	45	50	55	55	55	55	5-8
30		70	67	67	67	67	67	67	32-42
30	20	50	50	57	57	57	57	57	11-15
30	50	20	45	45	45	45	45	45	13-18

3.2.2 Prilling

Prilling was performed using prilling equipment developed by Peira (Turnhout, Belgium). The fatty acids (myristic and/or behenic acid) were molten and heated to 100 °C and MPT was added to the molten mixture under stirring. When MPT was completely dissolved, droplet formation was started. The mixture was fed towards a thermostated nozzle (90°C) by applying an air pressure of 0.5 bar. The drop time (i.e. the period during which the valve is open) was set at 0.07 s. The droplets formed at the needle (Ø 0.33 mm) were quench cooled in liquid nitrogen. The different compositions used for prilling are described in Table 3.2.

Table 3.2: Composition of the different mixtures used for prilling.

MPT (%)	Myristic acid (%)	Behenic acid (%)
		100
	28.57	71.43
	50	50
	71.43	28.57
30	20	50

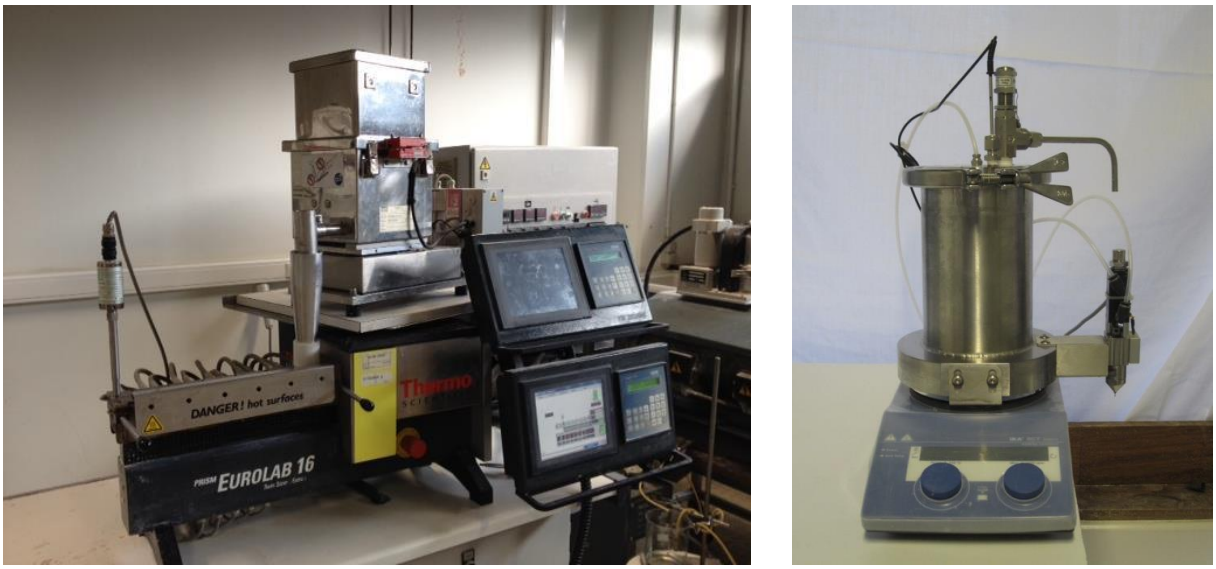

Figure 3.4: Pictures of the twin-screw extruder (left) and the prilling equipment (right) (60).

3.2.3 Storage

To study the influence of storage on drug release and solid state of the formulations, extrudates and prills containing 30% MPT, 20% myristic acid and 50% behenic acid and extrudates containing 30% MPT and 70% behenic acid were filled in hermetically sealed bags and stored in ovens of 25 °C and 40 °C. In vitro drug release testing, Raman and FT-IR spectroscopy, and MDSC were performed after 1 week, 1 month and 3 months.

3.2.4 In vitro drug release

A USP dissolution apparatus 1 (baskets) was used for the in vitro drug release testing of the different formulations. The equipment consisted of a VK 7010 dissolution system coupled with a VK 8000 automatic sampling station (Vankel, New Jersey, USA). The in vitro drug release was tested in triplicate on an amount of extrudates, respectively prills, corresponding to approximately 30 mg MPT. The rotational speed of the baskets was set at 100 rpm. The dissolution vessels were filled with 900 ml demineralized water, which was set at a temperature of 37 °C ± 0.5 °C.

Samples of 5 ml were automatically collected after 0.5 h, 1 h, 2 h, 4 h, 6 h, 8 h, 12 h, 16 h, 20 h and 24 h. The absorbance of the samples was measured at 222 nm using a double beam spectrophotometer (UV-1650 PC, Shimadzu, Antwerp, Belgium). MPT concentrations in the samples were calculated using the following calibration curve: $y = 28.117\ x + 0.0076$, where y and x are the absorbance and the concentration in mol/l, respectively.

The similarity between drug release profiles was evaluated using the similarity factor f_2, according to Shah et al. (61), and was calculated with the following equation:

$$f_2 = 50 log_{10}\left(\left[1 + \frac{1}{n}\sum_{t=1}^{n}(R_t - T_t)^2\right]^{-0.5} * 100\right)$$

where R_t and T_r are the cumulative drug release at each sample point of the reference and the test sample, respectively, and n is equal to the number of sample points. When multiple time points with a drug release higher than 85% are used in this similarity test, bias will occur. Therefore, no more than one sample point exceeding 85% drug release was considered in the calculation. Two drug release profiles are similar when the f_2 value is higher than 50, they are significantly different when the f_2 value is below 50 (61).

3.2.5 Modulated Differential Scanning Calorimetry (MDSC)

The thermal behaviour of the pure compounds, the physical mixtures and the corresponding formulations was evaluated using a differential scanning calorimeter Q2000 (TA Instruments, Zellik, Belgium) equipped with a cooling system. The DSC was calibrated using an indium standard. The samples (± 8 mg) were run in Tzero aluminum pans (TA Instruments, Zellik, Belgium). The temperature was increased from -20 °C up to 140 °C using a heating rate of 2 °C/min. The modulation period and amplitude were set at 60 s and 0.318 °C, respectively. The MDSC experiments were performed in a nitrogen atmosphere at a flow rate of 50 ml/min. Data analysis was performed with the Universal Analysis 2000 software version 4.5A (TA Instruments, New Castle, DA, USA). Melting temperatures and melting enthalpy were determined in the total heat flow signal.

3.2.6 Raman spectroscopy

Raman spectra of pure compounds, physical mixtures and formulations (extrudates and prills) were collected with a Raman Rxn1 spectrometer (Kaiser Optical Systems, Ann Harbour, MI, USA) to investigate their solid state behaviour. All spectra were recorded over the 0-1900 cm^{-1} range with a resolution of 4 cm^{-1} and an exposure time of 20 s. Collection and transfer of the data was automated using the HoloGRAMS^{TM} data collection software, the HoloREACT^{TM} reaction analysis and profiling software and the Matlab software. Data analysis was performed using the Simca software version 13.0.3 (Umetrics, Umeå, Sweden). All spectra were SNV-preprocessed.

3.2.7 Fourier Transform Infrared Spectroscopy

Fourier-Transform Infrared Spectroscopy (FT-IR) was performed on pure compounds, physical mixtures, extrudates and prills in order to identify intermolecular interactions. FT-IR spectra were recorded using a Nicolet iS5 FT-IR ATR spectrometer (Thermo Fischer Scientific, Waltham, MA, USA) by pressing the samples against a diamond ATR crystal. Spectra were collected between 4000 and 550 cm^{-1}. Each spectrum was the average of 16 scans with a resolution of 4 cm^{-1}. The data were analyzed using Simca software version 13.0.3 (Umetrics, Umeå, Sweden). All spectra were SNV-preprocessed.

3.2.8 X-ray diffraction (XRD)

To investigate crystallinity, X-ray diffraction was performed on the pure compounds, on the physical mixtures and on the corresponding extrudates and prills. X-ray diffraction was performed with a D5000 Cu KA diffractor (k = 1.54 Å) (Siemens, Karlsruhe, Germany) with a voltage of 40 mV in the angular range of $10° < 2\theta < 60°$, using a step scan mode (step size = 0.02°, counting time = 1s/step).

3.2.9 Scanning electron microscopy (SEM)

Samples were covered with a gold/palladium layer using a sputter coater (Auto Fine Coater, JF-C-1300, Jed, Tokyo, Japan). SEM images were recorded with an electron miscroscope (Jed J M 5600 LV, Jeol, Tokyo, Japan).

4 RESULTS AND DISCUSSION

4.1 EXTRUSION

Different mixtures of MPT and fatty acids were extruded using a co-rotating twin screw extruder. The composition of the formulations and the extrusion parameters are listed in Table 3.1. The die temperature was a critical parameter to obtain smooth extrudates. When this temperature was too low, the extrudates showed sharkskin, when it was too high, a paste was formed.

All formulations were extruded using a throughput of 0.3 kg/h, except for pure behenic acid. A throughput of 0.4 kg/h was necessary to ensure appropriate feeding of the screws when pure behenic acid was extruded. The extrudates of behenic acid were very brittle. The extrudates containing 30% MPT and 70% behenic acid and the extrudates containing 30% MPT, 20% myristic acid and 50% behenic acid showed less brittleness and had a smooth surface. Difficulties were encountered to extrude the mixture containing 30% MPT, 50% myristic acid and 20% behenic acid at high temperatures, because of the low melting temperature of myristic acid (54 °C).

4.2 PRILLING

The fatty acids were molten at 100 °C and MPT was added under stirring. A study of Vervaeck et al. indicated that MPT was not subject to thermal degradation when processed at 100 °C (21). MPT dissolved completely in the fatty acids at this temperature. The prills of pure behenic acid showed a high fragility. Better prills were obtained by adding drug and/or myristic acid. However, when the MA/BA ratio increased, the quality of the prills decreased.

4.3 IDENTIFICATION CHARACTERISTIC PEAKS

4.3.1 Raman spectroscopy

Fig. 4.1 illustrates the Raman spectra of MPT, behenic acid and the physical mixture containing 30% MPT and 70% behenic acid. Characteristic Raman bands of MPT could be found in the 630-650 cm^{-1}, 800-870 cm^{-1}, 920-980 cm^{-1} and 1200-1260 cm^{-1} regions. The peaks at 643 cm^{-1}, 821 cm^{-1}, 967 cm^{-1} and 1210 cm^{-1} could be assigned to an out of plane O-H vibration of the secondary alcohol, an out of plane O-H vibration of a carbonyl group, an O-H deformation vibration of the carboxyl group and C-N stretching respectively (21, 22, 62).

Characteristic bands of behenic acid were identified in the 870-920 cm^{-1}, 1055-1070 cm^{-1} and 1120-1140 cm^{-1}, and 1280-1310 cm^{-1} regions, caused by CH_2 rocking vibrations, C-C stretching vibrations and CH_2 twist vibrations, respectively (63).

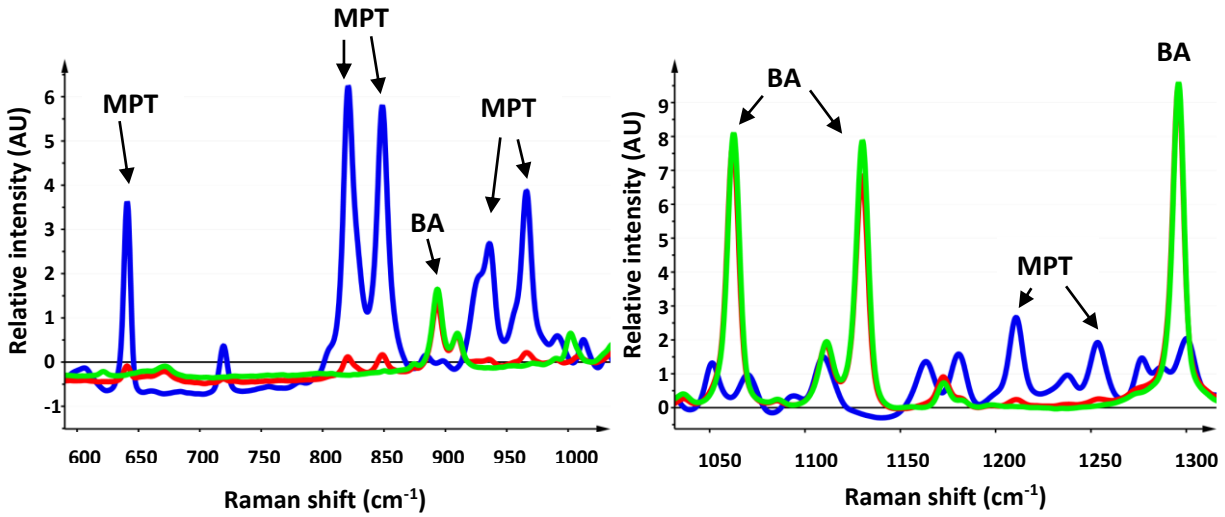

Figure 4.1: Raman spectra of MPT (blue), behenic acid (green) and the physical mixture containing 30% MPT and 70% behenic acid (red).

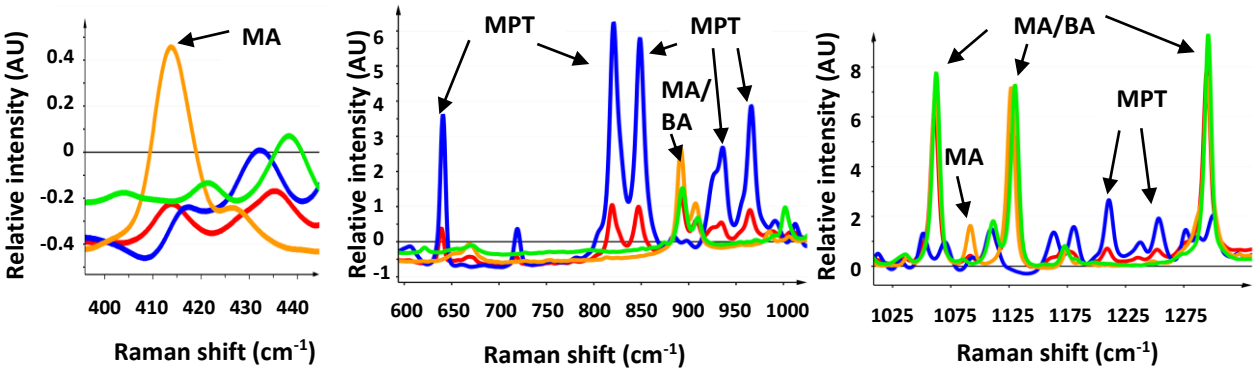

Figure 4.2: Raman spectra of MPT (blue), behenic acid (green), myristic acid (orange) and the physical mixture containing 30% MPT 20% myristic acid and 50% behenic acid (red).

Fig. 4.2 illustrates the Raman spectra of MPT, myristic acid, behenic acid and the physical mixture containing 30% MPT, 20% myristic acid and 50% behenic acid. Since myristic acid does not show overlapping peaks with MPT, the same characteristic Raman bands of MPT as described above, could be identified. However, due to their similar molecular structure, myristic acid and behenic acid could be hardly distinguished. Only two characteristic peaks for myristic acid were found at 413 cm^{-1} and 1092 cm^{-1}, caused by a chain expansion vibration shift and a C-C stretch vibration, respectively. Both peaks are the result of the difference in chain length of the fatty acids (63).

4.3.2 FT-IR analysis

The FT-IR spectra of MPT, behenic acid and the physical mixture containing 30% MPT and 70% behenic acid are illustrated in Fig.4.3. Characteristic FT-IR bands of MPT at 821 cm^{-1}, 1014 cm^{-1}, 1112 cm^{-1}, 1514 cm^{-1} and 1584 cm^{-1} represent an out of plane O-H vibration of the carbonyl group, a C-O deformation, a C-O symmetric stretching, a CO_2 asymmetric stretching and a CO_2 antisymmetric stretching, respectively (62). Characteristic bands of behenic acid were observed in the 1650-1750 cm^{-1} and 2800-2970 cm^{-1} regions and could be attributed to C=O stretching and CH_2 stretching vibration, respectively (21, 63, 64).

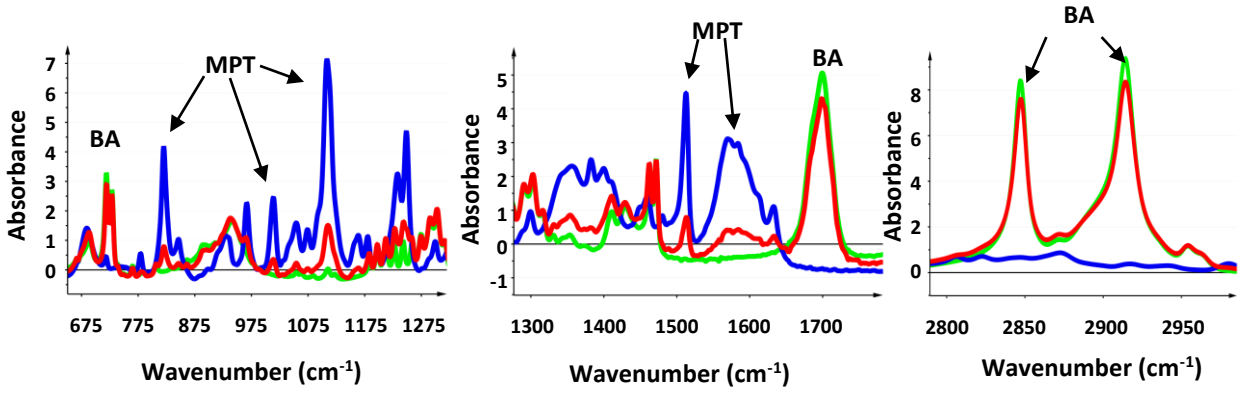

Figure 4.3: FT-IR spectra of MPT (blue), behenic acid (green) and a physical mixture containing 30% MPT and 70% behenic acid (red).

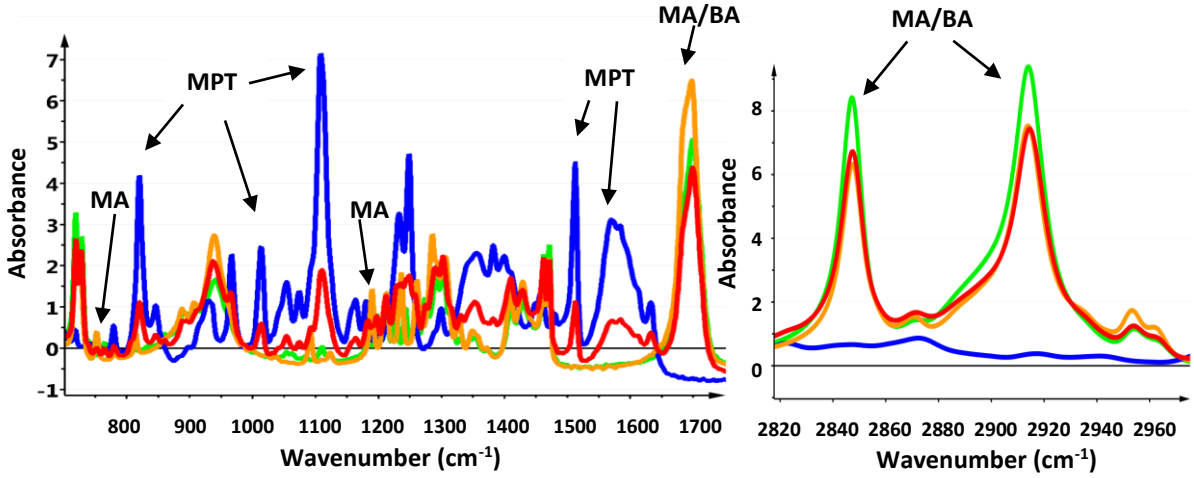

Figure 4.4: FT-IR spectra of MPT (blue), myristic acid (orange), behenic acid (green) and a physical mixture containing 30% MPT, 20% myristic acid and 50% behenic acid (red).

Fig. 4.4 illustrates the FT-IR spectra of MPT, myristic acid, behenic acid and the physical mixture containing 30% MPT, 20% myristic acid and 50% behenic acid. Since myristic acid does not show overlapping peaks with MPT, the same characteristic FT-IR bands of MPT as described above, could be identified. As already described for the Raman spectra, also the FT-IR spectra of myristic acid and behenic acid showed a lot of similarities. However, peaks in the 745-760 cm^{-1} and 1185-1195 cm^{-1} regions are specific for myristic acid.

4.4 COMPARISON BETWEEN EXTRUSION AND PRILLING

The temperature at the end of the extruder, the friction caused by the screws and the cooling conditions determine the solid state of the extrudate. Changes in solid state may influence the drug release (65). As prilling was performed at 100 °C and the droplets were finally quench cooled, the solid state may be influenced by the extreme process conditions. Therefore, the solid state of the formulations had to be examined.

Pure behenic acid, a 2:5 MA:BA mixture and a mixture containing 30% MPT, 20% myristic acid and 50% behenic acid were processsed via both extrusion and prilling. Extrudates and prills were examined using Raman spectroscopy, MDSC and X-ray diffraction in order to identify differences in solid state after extrusion and prilling. FT-IR spectroscopy was used to identify molecular interactions. The in vitro drug release rate was tested in order to investigate the influence of extrusion and prilling on the drug release rate of MPT.

4.4.1 Pure behenic acid

4.4.1.1 Raman spectroscopy

Fig. 4.5 illustrates the Raman spectra of unprocessed, extruded and prilled behenic acid. Extrusion was performed at 70 °C and 80 °C (i.e. below the melting point and around the melting point, respectively).

No differences were observed between the Raman spectra of pure behenic acid and the spectra of the prills and the extrudates. Moreover, the Raman spectra of behenic acid did not differ in function of extrusion temperature. These data suggested that the crystallinity of behenic acid was not affected by thermal processing.

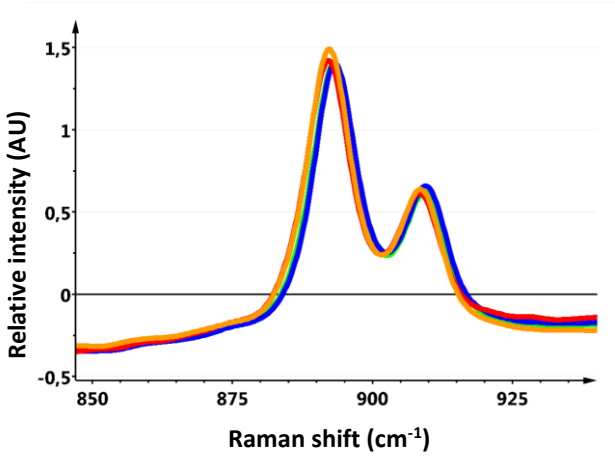

Figure 4.5: Raman spectra of behenic acid (red), behenic acid extrudates processed at 70 °C (green) and 80 °C (blue) and behenic acid prills (orange).

4.4.1.2 FT-IR analysis

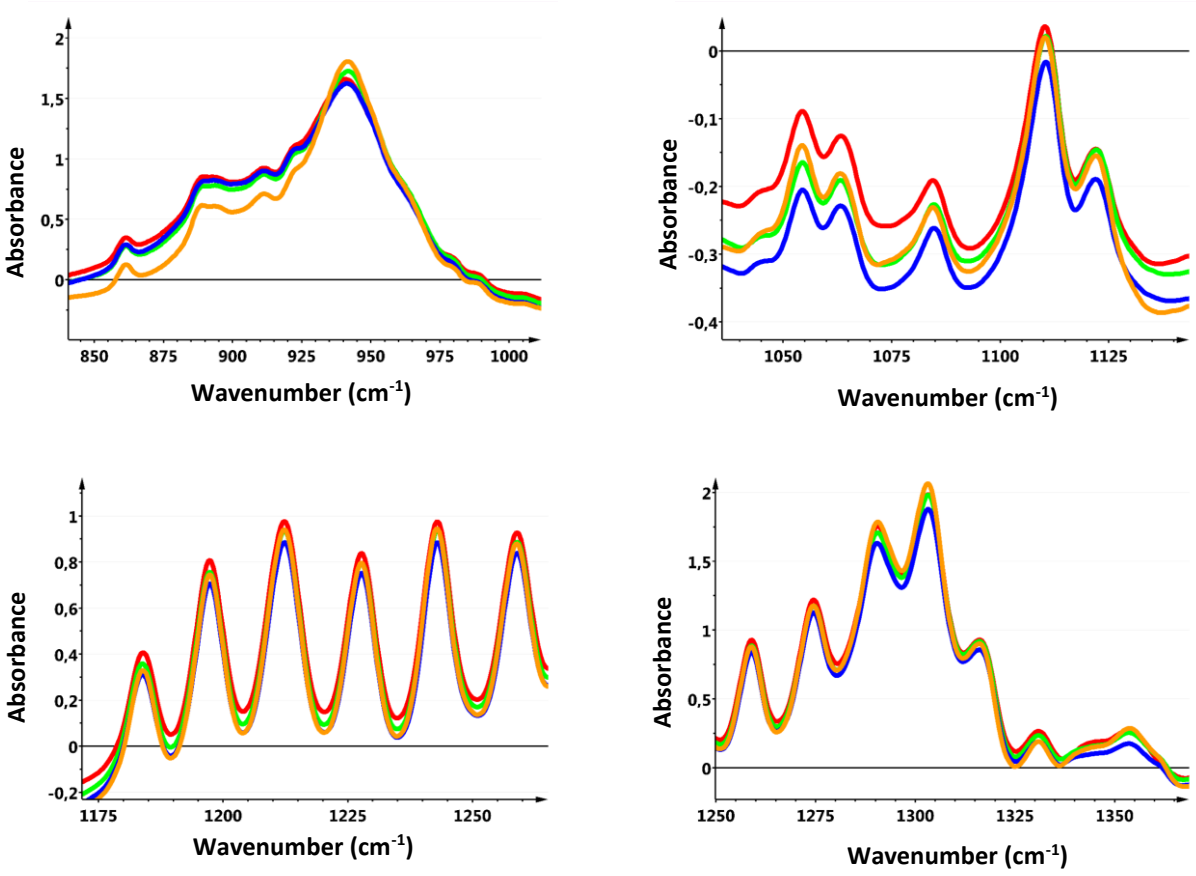

Figure 4.6: FT-IR spectra of behenic acid (red), behenic acid extrudates processed at 70 °C (green) and 80 °C (blue) and behenic acid prills (orange).

The FT-IR spectra of unprocessed behenic acid and extrudates and prills of behenic acid are presented in Fig. 4.6. However there was a weak change of the peak ratio of the vibration peaks in the 830-990 cm^{-1} region of the prills, no additional differences could be observed in the FT-IR spectra. The FT-IR spectra of the extrudates of behenic acid were similar to those of unprocessed behenic acid. As confirmed by Raman spectroscopy, extrusion and prilling did not alter the crystallinity of behenic acid.

4.4.1.3 MDSC

Table 4.1 lists the MDSC results of extruded and prilled behenic acid. The melting enthalpy, melt onset temperature and peak melting temperature of the melting endotherm of unprocessed behenic acid were 226.7 J/g, 74.69 °C and 77.95 °C, respectively. The onset and peak temperature of unprocessed and processed behenic acid were similar. The melting enthalpy of behenic acid processed at 80 °C was slightly increased compared to the enthalpy of the unprocessed behenic acid.

Table 4.1: Melting enthalpy, melt onset and peak melting temperature of behenic acid immediately after prilling and extrusion.

	Melting enthalpy (J/g)	Onset temperature (°C)	Peak temperature (°C)
Extrudates 70 °C	226.7	74.53	77.59
Extrudates 80 °C	232.7	75.09	77.67
Prills	223.9	74.85	77.74

4.4.1.4 Conclusion

Raman spectroscopy, FT-IR analysis and MDSC suggested that the crystallinity of behenic acid was not affected by thermal processing via prilling and extrusion.

4.4.2 2:5 MA:BA

4.4.2.1 Raman spectroscopy

Figure 4.7 illustrates the Raman spectra of the physical mixture containing 2:5 MA:BA and the corresponding extrudates and prills. Compared to the physical mixture, an additional peak showed up at 859 cm^{-1} in the spectra of the extrudates processed at 50 °C, 60 °C as well as 80 °C.

As this peak did not appear in the Raman spectra of extruded behenic acid (see 4.4.1.1), this phenomenon could probably be explained by molecular interactions between the fatty acids. Surprisingly, this peak did not appear after prilling. More intense mixing during extrusion can probably cause this difference.

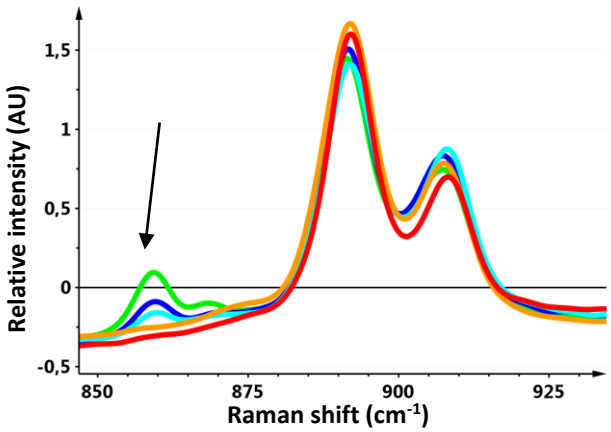

Figure 4.7: Raman spectra of the 2:5 MA:BA physical mixture (red), the corresponding extrudates processed at 50 °C (green), 60 °C (dark blue), 80 °C (light blue) and prills (orange).

4.4.2.2 FT-IR analysis

The FT-IR spectra of the physical mixture containing 2:5 MA:BA and corresponding extrudates and prills are shown in Fig. 4.8. The extrudates showed a modified peak ratio of the vibration peaks in the 920-960 cm^{-1} region (Fig. 4.8 A). These peaks could be attributed to OH-deformating vibrations in systems with hydrogen bonds. On the contrary, the prills showed in this region a big similarity with the physical mixture.

The 1100-1130 cm^{-1} band showed a changed peak ratio in the spectra of the extrudates (Fig. 4.8 B). Another difference was noticed in the 1220-1245 cm^{-1} region (Fig. 4.8 C), which could be attributed to C-O stretching in systems with hydrogen bonds (64). However, this change was less present in the prills. Since these changes were not observed in the FT-IR spectra of processed behenic acid, they were attributed to intermolecular interactions between the fatty acids.

The peak at 1290 cm^{-1}, attributed to C-O stretching, showed a shift to a lower wavenumber (i.e. 1287 cm^{-1}) in the extrudates in comparison with the physical mixture (Fig. 4.8 D), therefore suggesting that hydrogen bonds had been formed during extrusion. In the spectra of the prills, no peak shifts to a lower wavenumber were observed.

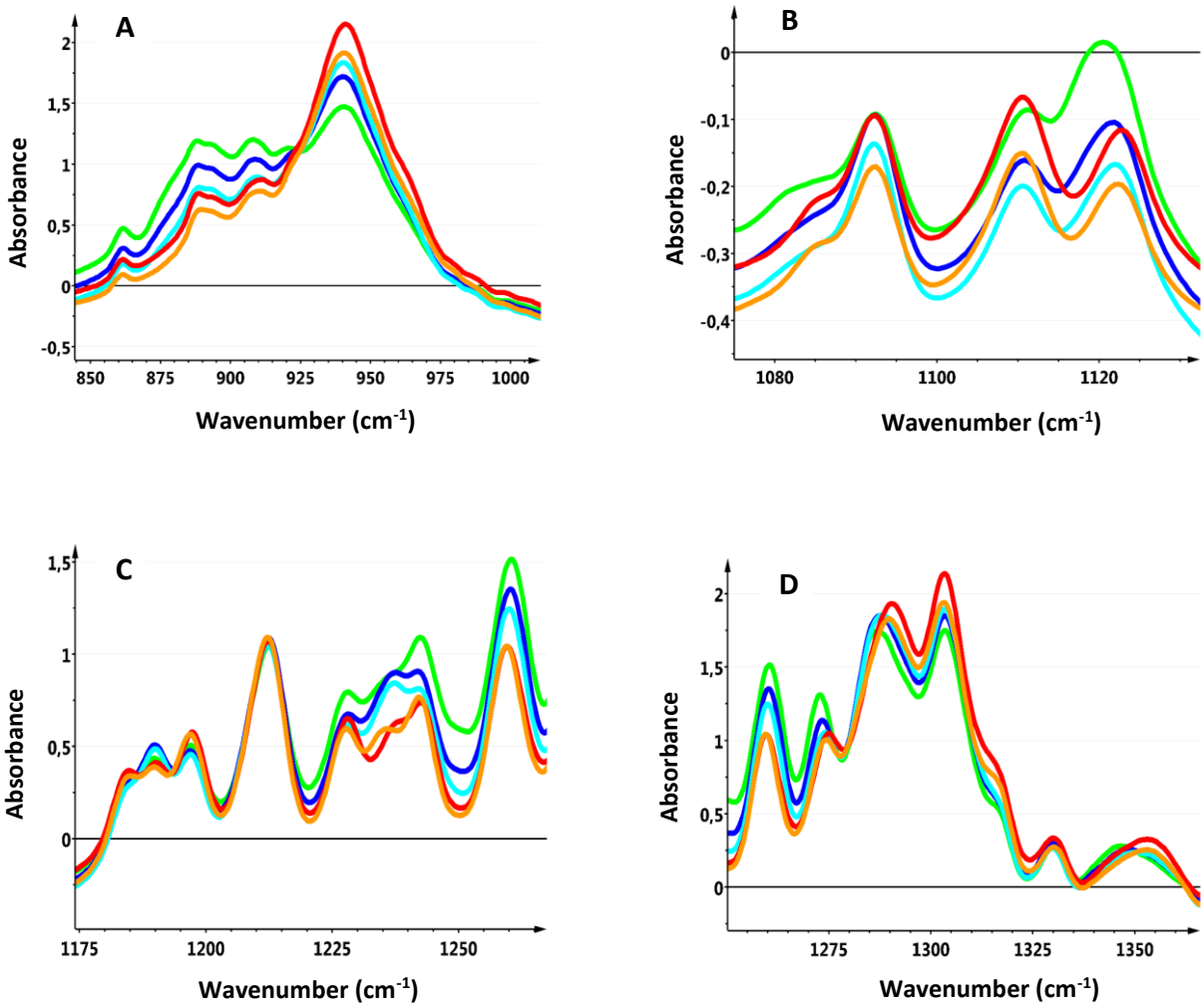

Figure 4.8: FT-IR spectra of the 2:5 MA:BA physical mixture (red), the corresponding extrudates processed at 50 °C (green), 60 °C (dark blue), 80 °C (light blue) and prills (orange).

In general, the FT-IR spectra of the prills showed more similarities to the physical mixture compared to the extrudates. More differences were noticed in the extrudates, suggesting a higher degree of interaction between the fatty acids during extrusion. A possible explanation was more intense mixing during extrusion caused by the screws.

4.4.2.3 MDSC

Table 4.2 illustrates the MDSC results of the pure compounds, the extrudates and prills containing 2:5 MA:BA and the corresponding physical mixture. Behenic acid and myristic acid, as received, were in a crystalline state. As the mixture contained 28.57% myristic acid and 71.43% behenic acid, the expected melting enthalpies for myristic acid and behenic acid were 57.1 J/g and 161.9 J/g, respectively. Therefore, the melting enthalpy of behenic acid was lower than expected in the physical mixture (128.4 J/g) and in the extrudates (131.9 J/g). On the other hand was the melting enthalpy of myristic acid higher than expected in the physical mixture (71.3 J/g) and in the extrudates (72.6 J/g).

The peak temperatures of myristic acid and behenic acid were significantly decreased in the physical mixture and in the extrudates compared to the unprocessed compounds. The peak melting temperature of myristic acid was decreased by 9 °C in the extrudates compared to unprocessed myristic acid. Yongcheng et al. suggested that a decrease in melting point may be the result of molecular interactions (66). The prills and extrudates had a different melting behaviour, as illustrated in Fig. 4.9. In the heat flow signal of the prills, there was no clear separation between the melting endotherms of myristic acid and behenic acid.

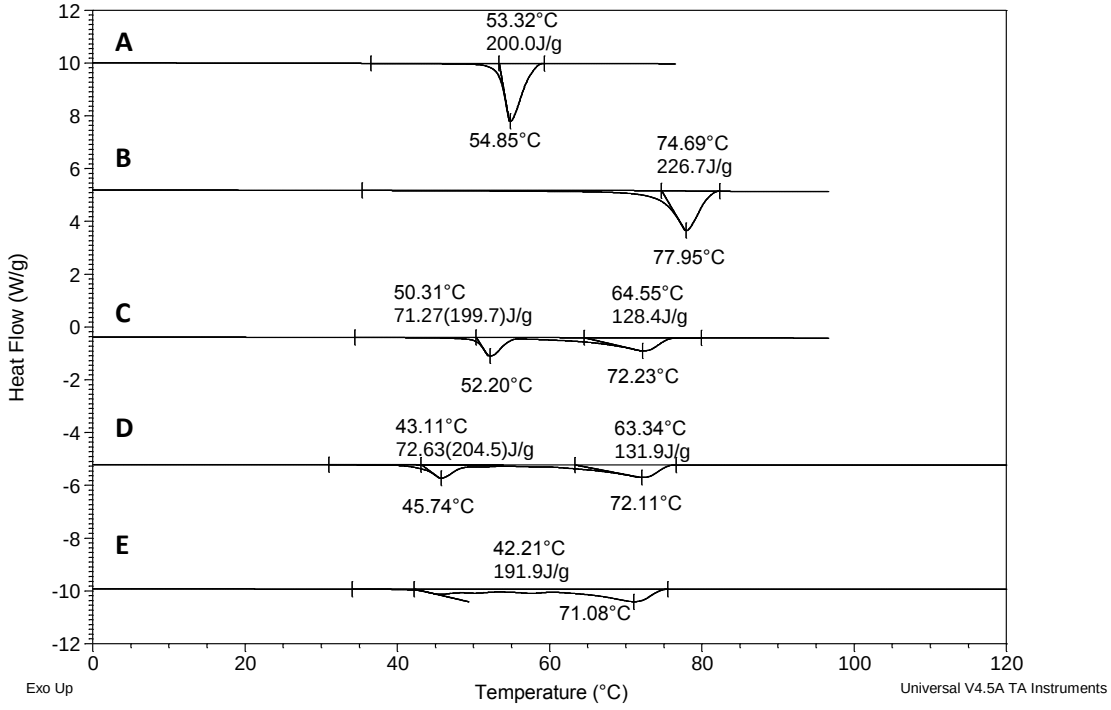

Figure 4.9: MDSC thermograms of myristic acid (A), behenic acid (B), 2:5 MA:BA physical mixture (C), corresponding extrudates extruded at 80 °C (D) and prills (E).

Table 4.2: Melting enthalpy and peak melting temperature of the 2:5 MA:BA physical mixture and the corresponding extrudates and prills.

	Melting enthalpy (J/g)		Peak temperature (°C)	
	MA	**BA**	**MA**	**BA**
Physical mixture	71.3	128.4	50.3	72.2
Extrudates 80 °C	72.6	131.9	45.7	72.1
Prills	191.9		42.2	

4.4.2.4 X-ray diffraction

The X-ray patterns of unprocessed myristic and behenic acid, the 2:5 MA:BA physical mixture and the corresponding extrudates and prills are shown in Fig. 4.10. Behenic acid showed representative peaks for 2θ at 13.0° and 16.7°. These peaks had almost completely disappeared in the prills, indicating loss of crystallinity of behenic acid. However, this was not confirmed by the Raman spectra. The same observation could be made for myristic acid (representative peak for 2θ at 14.3°).

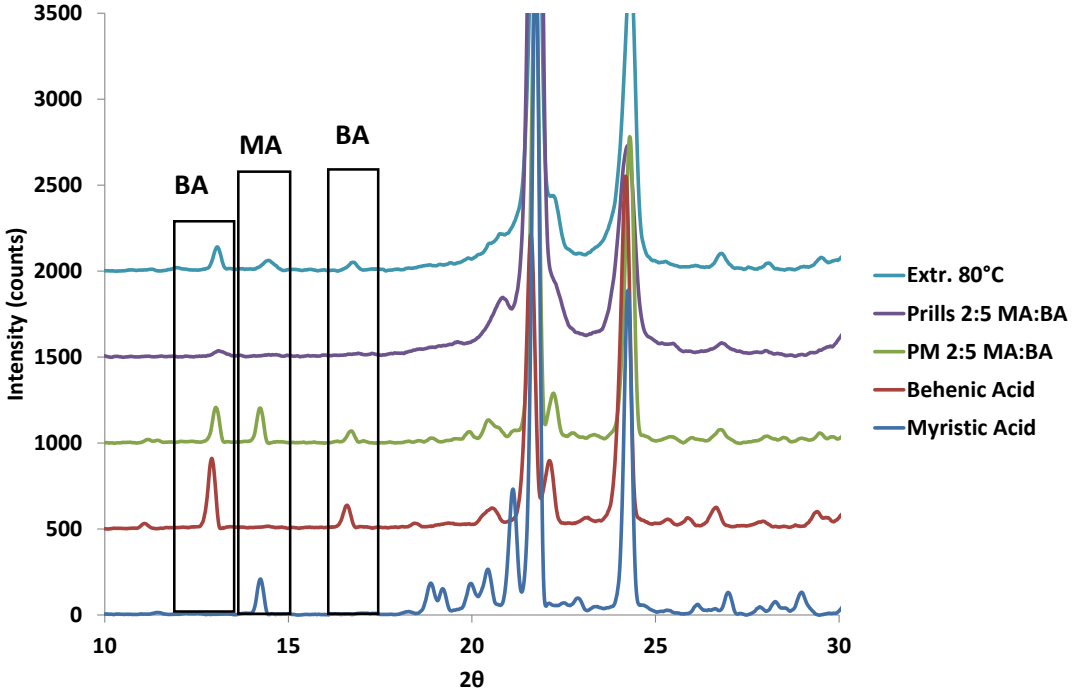

Figure 4.10: X-ray patterns of myristic acid (dark blue), behenic acid (red), the 2:5 MA:BA physical mixture (green), the corresponding prills (purple) and extrudates processed at 80 °C (light blue).

4.4.2.5 Conclusion

Raman spectroscopy and FT-IR analysis suggested that molecular interactions between the fatty acids occurred during extrusion. The Raman and FT-IR spectra of the prills were more similar to the physical mixture compared to the extrudates, which could probably be explained by more intense mixing during extrusion.

4.4.3 30% MPT 20% MA 50% BA

4.4.3.1 In vitro drug release

Figure 4.11 represents the drug release profiles for prills and extrudates containing 30% MPT, 20% myristic acid and 50% behenic acid. Combination of myristic acid and behenic acid as matrix formers resulted in a controlled drug release. After 24 h, 83% and 77% of the total drug load was released out of the extrudates and the prills, respectively. As previously explained in section 3.2.4, the similarity between dissolution profiles was evaluated using the similarity factor f_2. Even though the prills had a higher contact area, there was no significant difference between the drug release profiles of the extrudates and the prills, as indicated by the f_2 value ($f_2 > 50$). However, not only the contact area, but also the diffusion coefficient D is an important factor influencing the drug release profile (44).

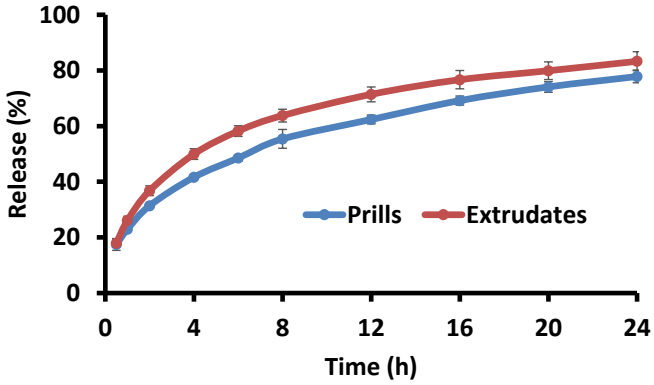

Figure 4.11: In vitro drug release profiles of 30:20:50 MPT:MA:BA extrudates (red) and prills (blue).

4.4.3.2 Raman spectroscopy

The extrudates were processed at 57 °C, which was higher than the melting temperature of myristic acid (54°C), but lower than the melting temperature of behenic acid (80°C). The prills were processed at 100 °C, above the melting temperatures of both myristic acid and behenic acid. Fig. 4.12 shows the Raman spectra of the 30:20:50 MPT:MA:BA physical mixture and the corresponding extrudates and prills.

Crystalline MPT in the extrudates could be proven based on its characteristic bands in the 800-870 cm^{-1}, 920-980 cm^{-1} and 1200-1260 cm^{-1} regions. The specific peaks of MA/BA (870-920 cm^{-1}, 1055-1070 cm^{-1} and 1120-1140 cm^{-1}) and the characteristic myristic acid bands (405-420 cm^{-1} and 1185-1195 cm^{-1}) were present in the extrudates, confirming their highly crystalline state. After extrusion, the Raman spectra showed an additional peak at 859 cm^{-1}. This peak was also detected in the 2:5 MA:BA extrudates (see 4.4.2.1). The peak did not appear after prilling.

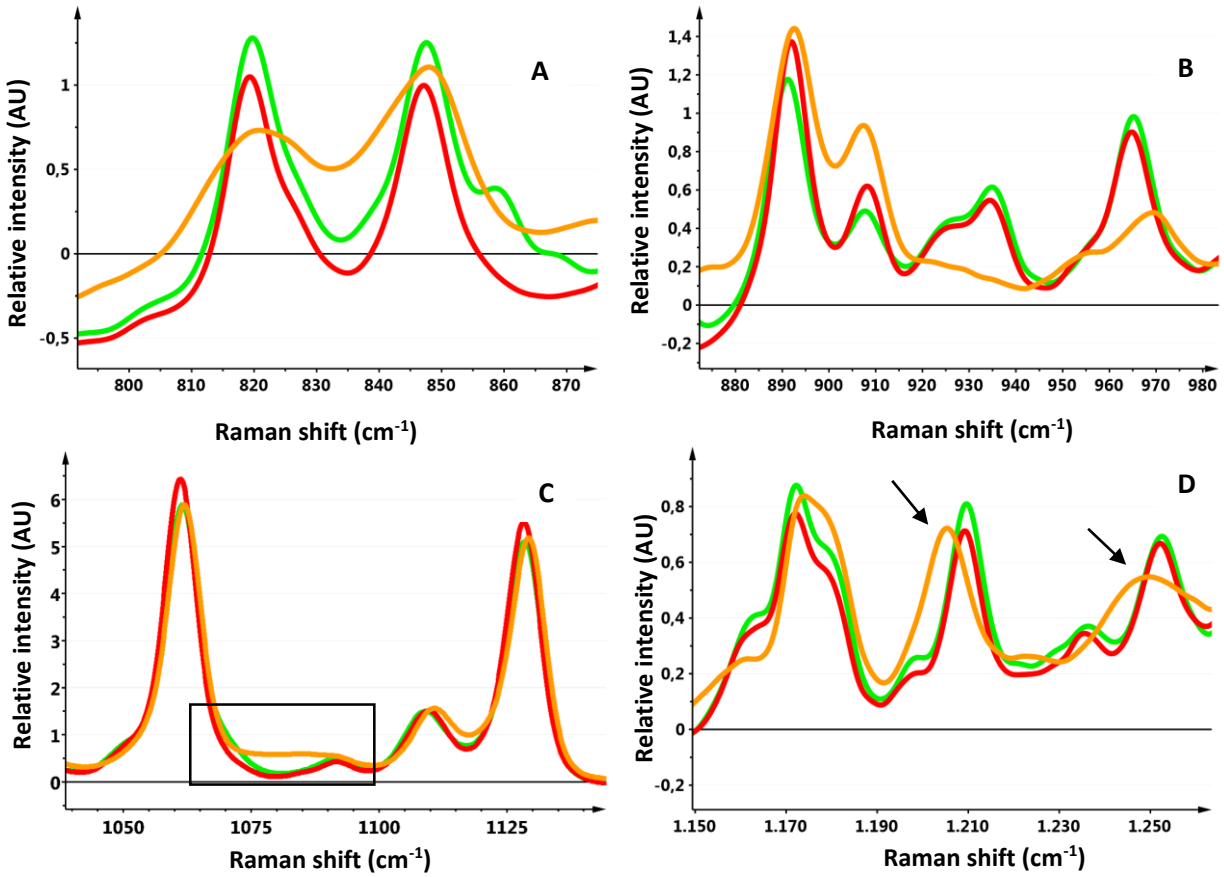

Figure 4.12: Raman spectra of extrudates (green), prills (orange) and the physical mixture (red) containing 30% MPT, 20% MA and 50% BA.

The bands in the 800-860 cm^{-1} and 1200-1260 cm^{-1} regions had broadened and the band in the 920-970 cm^{-1} region had almost disappeared (Fig. 4.12 A, B and D) in the Raman spectra of the prills. As these bands were specific for MPT, these results indicated a loss in crystallinity during prilling and the presence of an amorphous MPT fraction. Although the crystallinity of the drug was decreased in the prills relative to the extrudates, the in vitro drug release profile of MPT was not affected (see 4.4.3.1).

Prilling also induced a broadening of the specific myristic acid peaks at 1092 cm^{-1} (Fig. 4.12 C) and 413 cm^{-1} (data not shown), indicating less crystalline myristic acid. In the spectra of the prills, the peaks at 1210 cm^{-1} and 1252 cm^{-1} were shifted to a lower wavenumber (i.e. 1205 cm^{-1} and 1249 cm^{-1}, respectively) (Fig. 4.12 D). These shifts could be possibly attributed to intermolecular interactions between MPT and the fatty acids. Since these interactions did not appear after extrusion, the higher process temperature and the molten state of the fatty acids during prilling enabled these interactions.

4.4.3.3 FT-IR analysis

Fig. 4.13 shows the FT-IR bands for the 30:20:50 MPT:MA:BA physical mixture and the corresponding formulations. The FT-IR peak in the 800-850 cm^{-1} region had broadened in the prills (Fig. 4.13 A), suggesting a decrease in crystallinity of MPT during prilling.

The 1220-1320 cm^{-1} band could be attributed to both MPT and the fatty acids. In the extrudates and prills, there was a change in ratio in this band, indicating intermolecular interactions between MPT and the fatty acids (Fig. 4.13 C). Similar observations were made for the 875-975 cm^{-1} band (Fig. 4.13 B). However, in that band, the prills were more similar to the physical mixture compared to the extrudates. A change in peak ratio in the 875-975 cm^{-1} band was observed in the 2:5 MA:BA extrudates as well (see 4.4.2.2), suggesting hydrogen bond formation between the fatty acids and probably between MPT and the fatty acids as well.

The bands in the 1220-1260 cm^{-1} region, attributed to both MPT and the fatty acids, appeared sharpened in the extrudates and broadened in the prills compared to the physical mixture. The peaks at 1275 cm^{-1} and 1289 cm^{-1} were specific for the fatty acids (C-O stretching) and showed a shift to a lower wavenumber in the extrudates (i.e. 1273 cm^{-1} and 1286 cm^{-1}, respectively) compared to the physical mixture, indicating molecular interactions between the fatty acids (Fig. 4.13 C). The same observation was made in the 2:5 MA:BA extrudates.

The FT-IR band at 1410 cm^{-1}, caused by O-H bending and attributed to both MPT and the fatty acids, was shifted to a lower wavenumber (i.e. 1406 cm^{-1}) in the extrudates and was broadened in both extrudates and prills (Fig. 4.13 D). Therefore, these results indicated

intermolecular interactions between MPT and the fatty acids in the extrudates and a decreased crystallinity in both extrudates and prills.

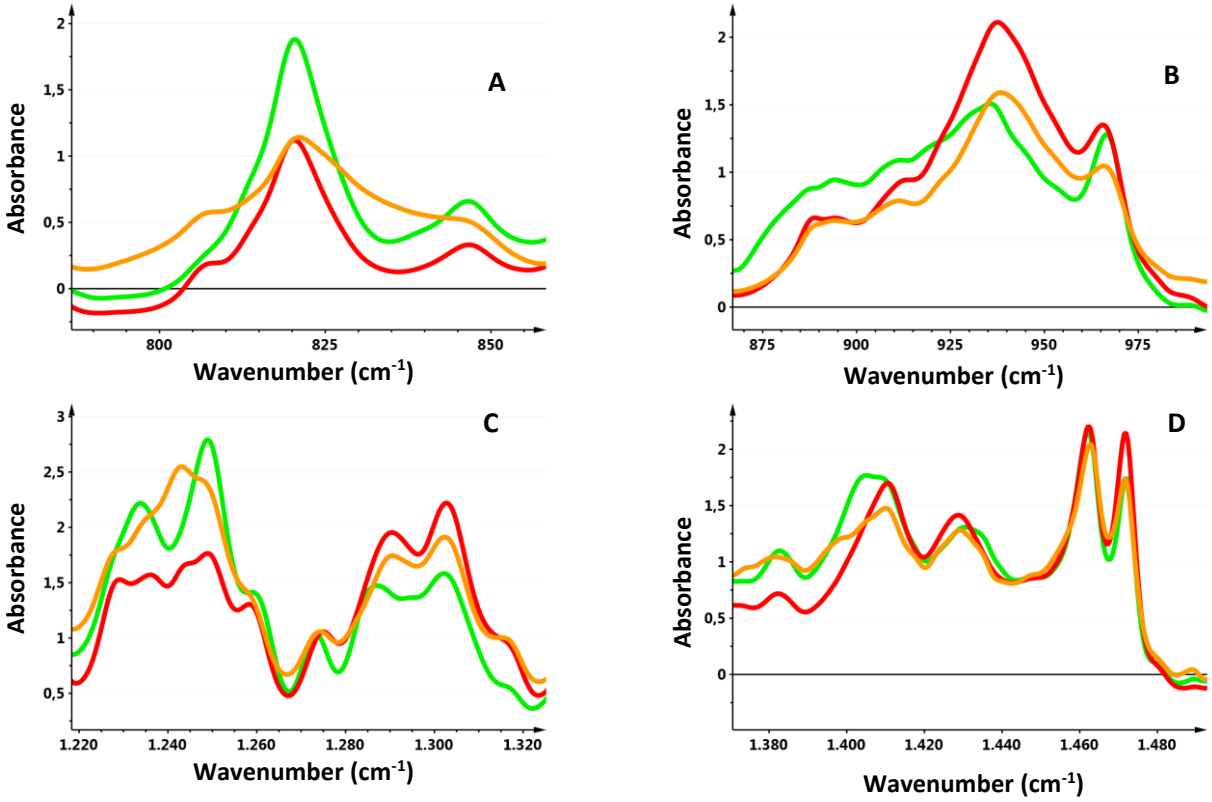

Figure 4.13: FT-IR spectra of extrudates (green), prills (orange) and the physical mixture (red) containing 30% MPT, 20% MA and 50% BA.

4.4.3.4 MDSC

The melting enthalpy and the peak melting temperature of the 30:20:50 MPT:MA:BA extrudates and prills are listed in Table 4.3. The fact that no melting endotherm of MPT was revealed in the physical mixture and the formulations could be explained by dissolution of MPT in the molten fatty acids (22).

Table 4.3: Melting enthalpy and peak melting temperature of 30:20:50 MPT:MA:BA extrudates and prills immediately after manufacturing.

	Melting enthalpy (J/g)		Peak temperature (°C)	
	MA	**BA**	**MA**	**BA**
Physical mixture	57.1	82.9	52.3	71.3
Extrudates	43.3 ± 0.3	113.9 ± 0.7	42.8 ± 0.1	69.0 ± 0.1
Prills	137.7 ± 3.1		68.2 ± 0.1	

MPT, behenic acid and myristic acid, as received, were in a crystalline state. The formulation contained 20% myristic acid and 50% behenic acid. Therefore, the expected melting enthalpies for myristic acid and behenic acid were 40 J/g and 113.4 J/g, respectively. These values corresponded with the melting enthalpies in the extrudates, suggesting that the crystallinity of the fatty acids was not affected by processing via extrusion.

The peak melting temperatures of myristic acid and behenic acid had decreased in the physical mixture and in the extrudates compared to the pure compounds, indicating interactions between the fatty acids and/or between MPT and the fatty acids. The peak melting temperature of myristic acid was decreased by 12 °C in the extrudates compared to unprocessed myristic acid.

Prills and extrudates showed a significantly different melting behaviour as presented in Fig. 4.14. The melting endotherm of the extrudates showed separation between the myristic and behenic acid peak, while there was no peak separation in the prills. The total melting enthalpy in the prills (137.7 J/g) was lower than the expected value (153.4 J/g).

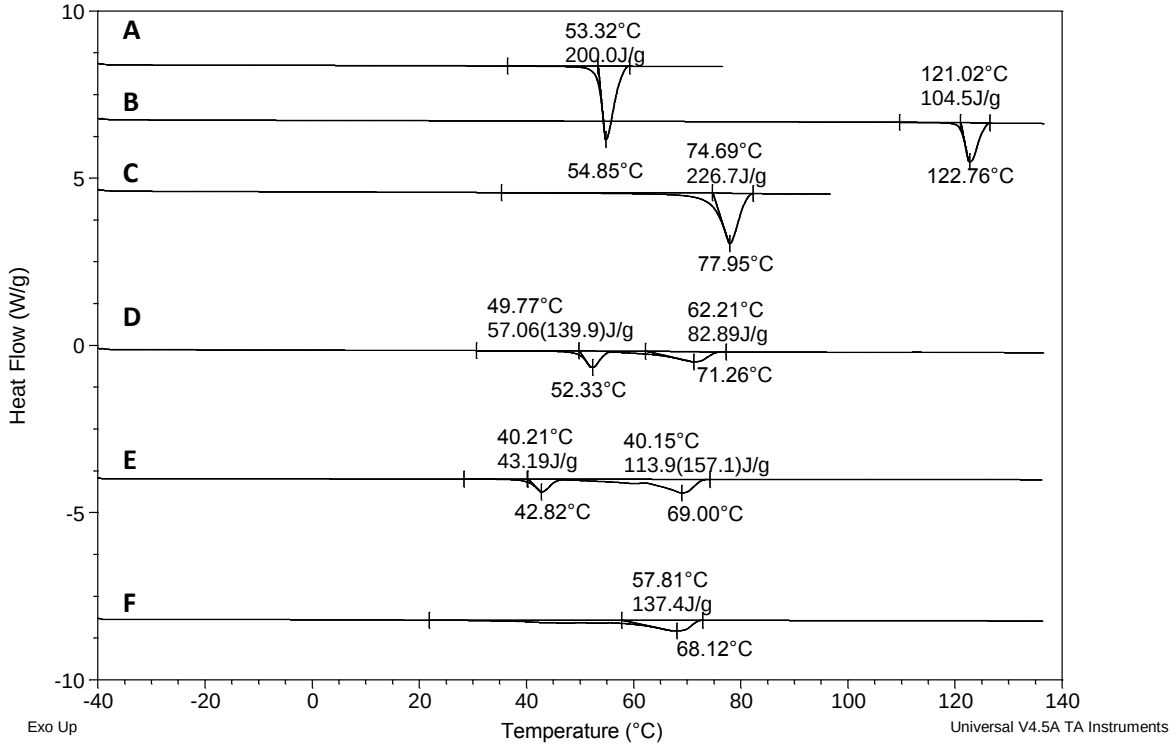

Figure 4.14: MDSC thermograms of myristic acid (A), MPT (B), behenic acid (C), the 30:20:50 MPT:MA:BA physical mixture (D) and the corresponding extrudates (E) and prills (F).

4.4.3.5 X-ray diffraction

Fig. 4.15 shows the X-ray patterns of MPT, myristic acid, behenic acid and the 30:20:50 MPT:MA:BA extrudates and prills. No differences could be observed, therefore suggesting that the extrudates and the prills had the same degree of crystallinity. These data were not in agreement with the results of Raman spectroscopy, where peak broadening in the prills indicated a less crystalline state of MPT and myristic acid. However, the XRD patterns of MPT and myristic acid showed overlapping peaks, what made it more difficult to detect changes in solid state of these compounds.

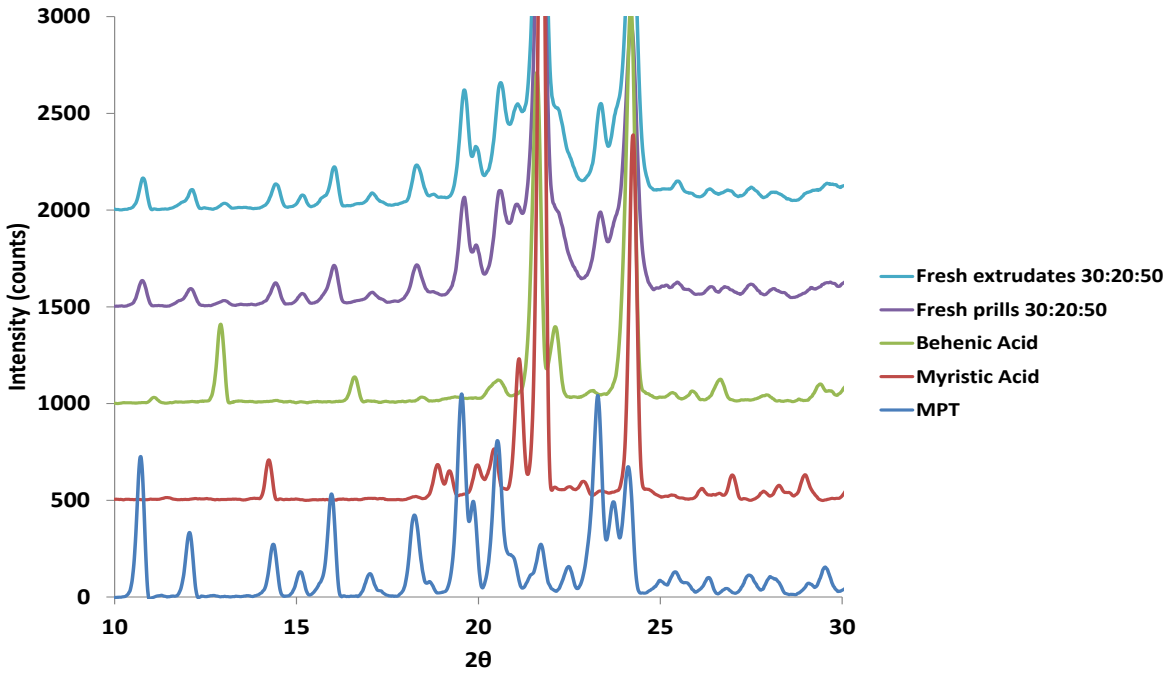

Figure 4.15: X-ray patterns of the 30:20:50 MPT:MA:BA extrudates (light blue), prills (purple), MPT (dark blue), myristic acid (red) and behenic acid (green).

4.4.3.6 Scanning electron microscopy

The SEM images of 30:20:50 MPT:MA:BA prills and extrudates are shown in Fig. 4.16. The images of the formulations were recorded using the same magnification (2000 x). The SEM image of MPT showed needle-like crystals (Fig. 4.16 A), while behenic acid had a lamellar structure (Fig. 4.16 B).

The prills represented a smoother surface compared to the extrudates. No MPT crystals could be seen at the surface, suggesting that MPT was completely dissolved in the fatty acids. Before the prilling process was initiated, MPT was completely dissolved in the molten fatty acids yielding a more homogeneous matrix.

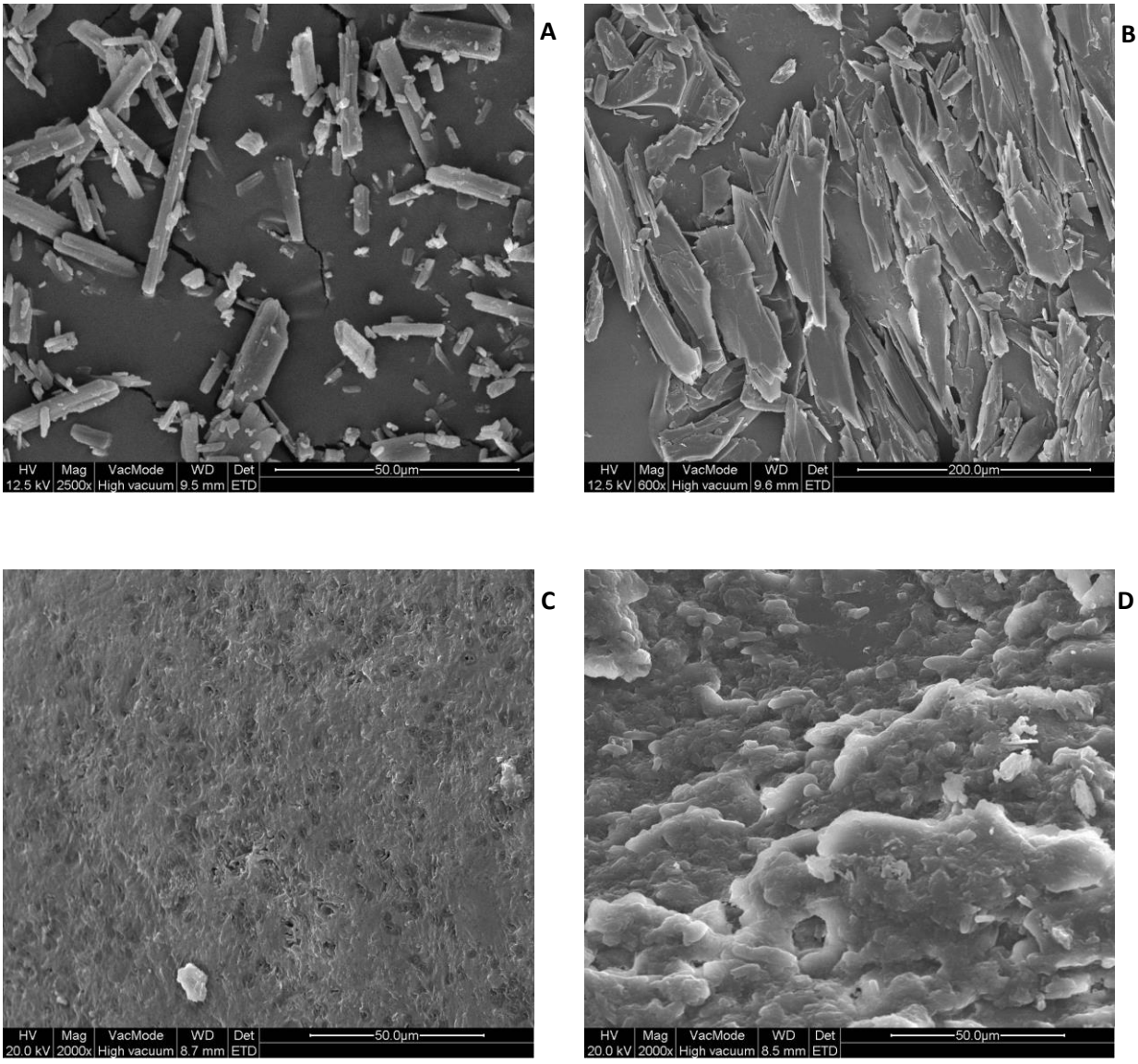

Figure 4.16: SEM images of MPT (A), behenic acid (B), 30:20:50 MPT:MA:BA prills (C) and extrudates processed at 80 °C (D).

4.4.3.7 Conclusion

A controlled release formulation could be obtained by adding a certain percentage of myristic acid to the formulation. The slower release rate could be explained by interactions between the fatty acids and/or between MPT and the fatty acids.

4.4.4 30% MPT 70% BA

4.4.4.1 In vitro drug release

Fig. 4.17 represents the in vitro drug release profile of extrudates containing 30% MPT in a behenic acid matrix. After 4 h, 86% of the total drug load was released and a complete release was obtained after 12 h. Surprisingly, as a faster release was expected in the formulations containing myristic acid, the release rate was significantly faster in the 30:70 MPT:BA extrudates in comparison with the 30:20:50 MPT:MA:BA formulations (see 4.4.3.1).

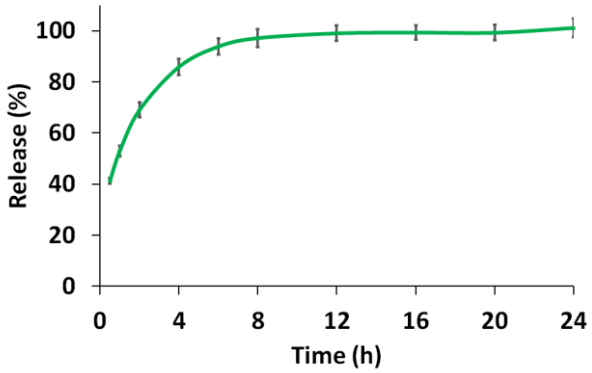

Fig. 4.17: In vitro drug release of 30:70 MPT:BA extrudates immediately after processing.

4.4.4.2 Raman spectroscopy

The extrudates were processed at 67 °C, i.e. below the melting temperature of behenic acid. The Raman spectra of the fresh extrudates and the physical mixture were similar, therefore suggesting that MPT is in the crystalline form after extrusion (spectra not shown).

The study by Vervaeck et al. (2013) mentioned a peak broadening in the 800-875 cm^{-1} region in the Raman spectra of the prills. Moreover, MPT specific peaks had almost disappeared in the 920-980 cm^{-1} region of the prills compared to the spectra of the physical mixture (22). These changes were not detected in the Raman spectra of the extrudates, indicating that the solid state of MPT was more crystalline in the extrudates in comparison with the prills.

4.4.4.3 FT-IR analysis

The FT-IR spectra (Fig. 4.18) showed a changed ratio of the vibration peaks in the 1220-1260 cm^{-1} region of the extrudates compared to the spectra of the physical mixture. The peak at 1249 cm^{-1} (attributed to mainly MPT) represented an O-H deformation (62). The change in

ratio suggested an interaction between MPT and behenic acid. Even though the Raman spectra indicated that MPT was mainly in the crystalline form, this changed ratio suggests that interactions had occurred during extrusion.

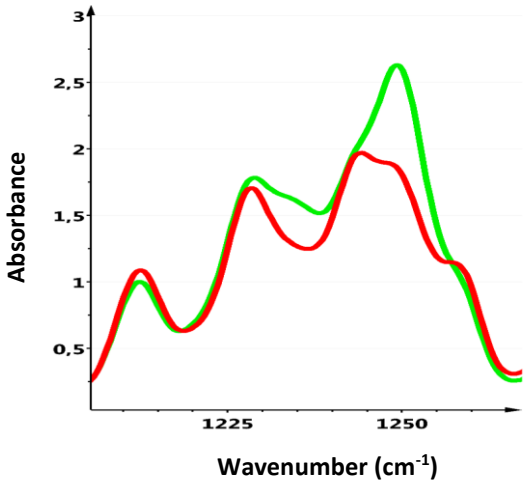

Figure 4.18: FT-IR spectra of the 30:70 MPT:BA physical mixture and the corresponding formulation.

4.4.4.4 MDSC

The melting enthalpy, melt onset temperature and peak melting temperature of the 30:70 MPT:BA physical mixture and the corresponding formulation are shown in Table 4.4. As the formulation contained 70% behenic acid, a melting enthalpy of 158.7 J/g was expected for behenic acid. The melting enthalpy of behenic acid in the extrudates (183.7 J/g) was higher than expected.

Similar observations were made in a previous study by Vervaeck et al., where the thermal behaviour of prills containing 30% MPT and 70% behenic acid was studied. It was suggested that the excess of energy was necessary to dissolve the MPT crystals (22).

Table 4.4: Melting enthalpy, melt onset and peak melting temperature of 30:70 MPT:BA extrudates and prills immediately after manufacturing.

	Melting enthalpy (J/g)	Onset temperature (°C)	Peak temperature (°C)
Physical mixture	142.0	73.7	76.7
Extrudates	183.7 ± 2.6	72.3 ± 0.1	74.8 ± 0.1

4.4.4.5 X-ray diffraction

Fig. 4.19 shows the X-ray patterns of the 30:70 MPT:BA physical mixture and the corresponding extrudates and prills. The peak in the XRD pattern of the prills in the 19°-20° (2θ) region (attributed to MPT) was broadened and less peak separation was observed in the prills compared to the extrudates and the physical mixture. These results confirmed our previous assumption that the extrudates contained more crystalline MPT compared to the prills.

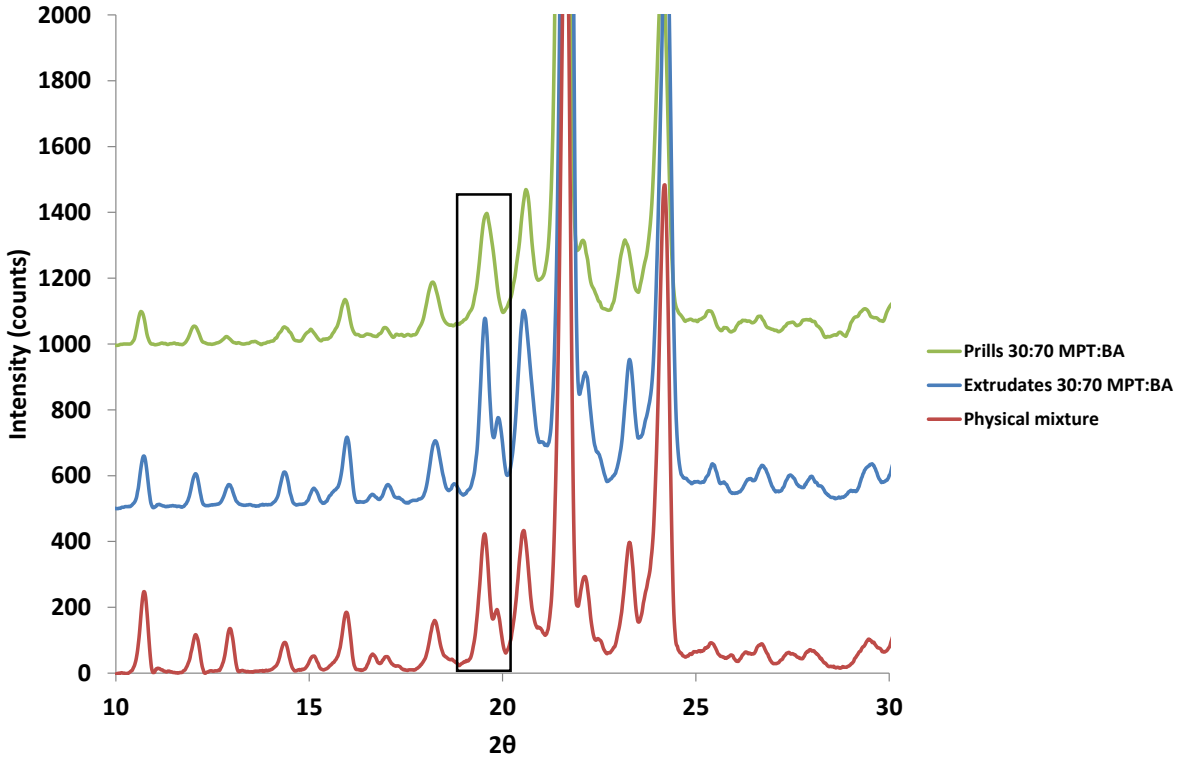

Figure 4.19: X-ray diffraction patterns of the 30:70 MPT:BA physical mixture (red) and the corresponding extrudates (blue) and prills (green).

4.4.4.6 Scanning electron microscopy

SEM analysis of the extrudates and prills (Fig. 4.20) revealed that the extrudates processed at 80 °C and the prills had a smoother surface compared to the extrudates processed at 63 °C. These results suggested that a higher processing temperature generated a smoother surface.

Crystalline MPT had a needle-shaped form on SEM images. MPT was visible on the SEM image of the extrudates processed at 63 °C (Fig. 4.20 A), but not on the surface of the extrudates processed at 80 °C (Fig. 4.20 B). These results suggested that more MPT was dissolved in the behenic acid matrix at a higher processing temperature. No MPT crystals could be seen on the surface of the prills (Fig. 4.20 C) due to the fact that all MPT was dissolved in the molten behenic acid before the prilling process was started.

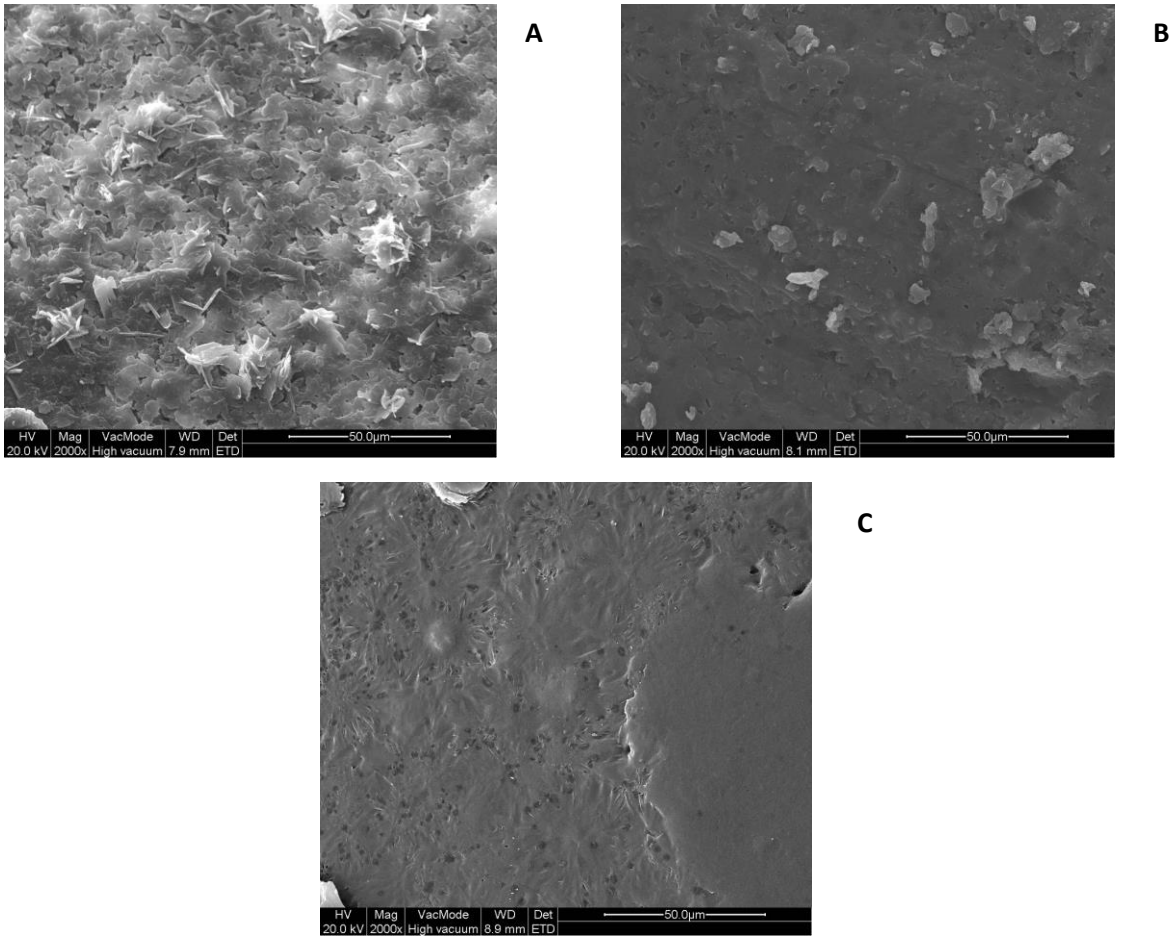

Figure 4.20: SEM images of the surface of 30:70 MPT:BA extrudates produced at 63 °C (A), 80 °C (B) and prills (C).

4.4.4.7 Conclusion

The drug release out of the 30:70 MPT:BA extrudates was significantly faster compared to the 30:20:50 MPT:MA:BA formulations. Raman spectroscopy and MDSC suggested that both MPT and behenic acid were in the crystalline state after extrusion. However, FT-IR spectroscopy indicated that molecular interactions occurred between MPT and behenic acid.

4.5 STABILITY STUDY

Drug release out of lipid carriers can change during storage (22, 31, 35, 38). Therefore, the physical stability of the extrudates and prills containing 30% MPT, 20% myristic acid and 50% behenic acid and the extrudates containing 30% MPT in a behenic acid matrix was investigated. Extrudates and prills were stored, immediately after processing, in hermetically sealed bags at 25 °C and 40 °C during 3 months. In vitro drug release rate and solid state were analyzed after 1 week, 1 month and 3 months storage.

4.5.1 Extrudates 30% MPT 20% MA 50% BA

4.5.1.1 In vitro drug release

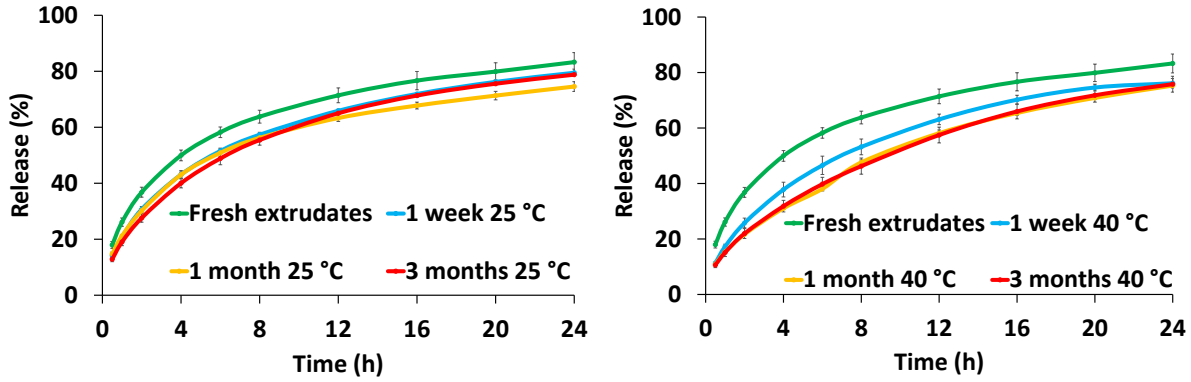

Fig. 4.21: Drug release profiles of fresh extrudates (green) and extrudates stored during 1 week (blue), 1 month (yellow) and 3 months (red) at 25 °C (left) and 40 °C (right).

The influence of storage on drug release is shown in Fig. 4.21. Drug release profiles remained similar during storage at 25 °C (f_2 values ranging between 56 and 63). However, drug release after 1 month and 3 months storage at 40 °C was decreased compared to the freshly prepared extrudates ($f_2 < 50$). Drug release profiles obtained after 1 month and 3 months storage at 40 °C were not significantly different ($f_2 > 50$), but differed significantly from the freshly prepared formulation ($f_2 < 50$). Raman and FT-IR spectroscopy, MDSC and X-ray diffraction were performed in order to find an explanation for these differences.

4.5.1.2 Raman spectroscopy

After extrusion of the 30% MPT, 20% MA and 50% BA mixture, a new peak showed up in the Raman spectrum at 859 cm^{-1} (see 4.4.2.1). This peak remained after storage at 40 °C, as shown in Fig. 4.22. Identical observations were made during storage at 25 °C (data not shown).

After 1 week, 1 month and 3 months storage at 25 °C and 40 °C, the Raman spectra were equal to those of the fresh formulation (data not shown), suggesting that the solid state of MPT and the fatty acids did not change during storage. However, solid state testing after 6 months and 1 year is necessary to ensure the stability of the extrudates.

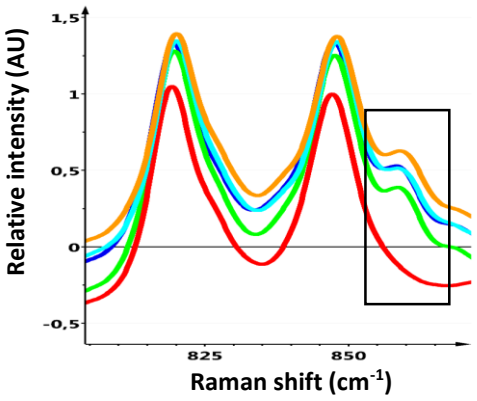

Fig. 4.22: Raman spectra of 30:20:50 MPT:MA:BA physical mixture (red), fresh extrudates (green), 1 week (dark blue), 1 month (orange) and 3 months (light blue) storage at 40 °C.

4.5.1.3 FT-IR analysis

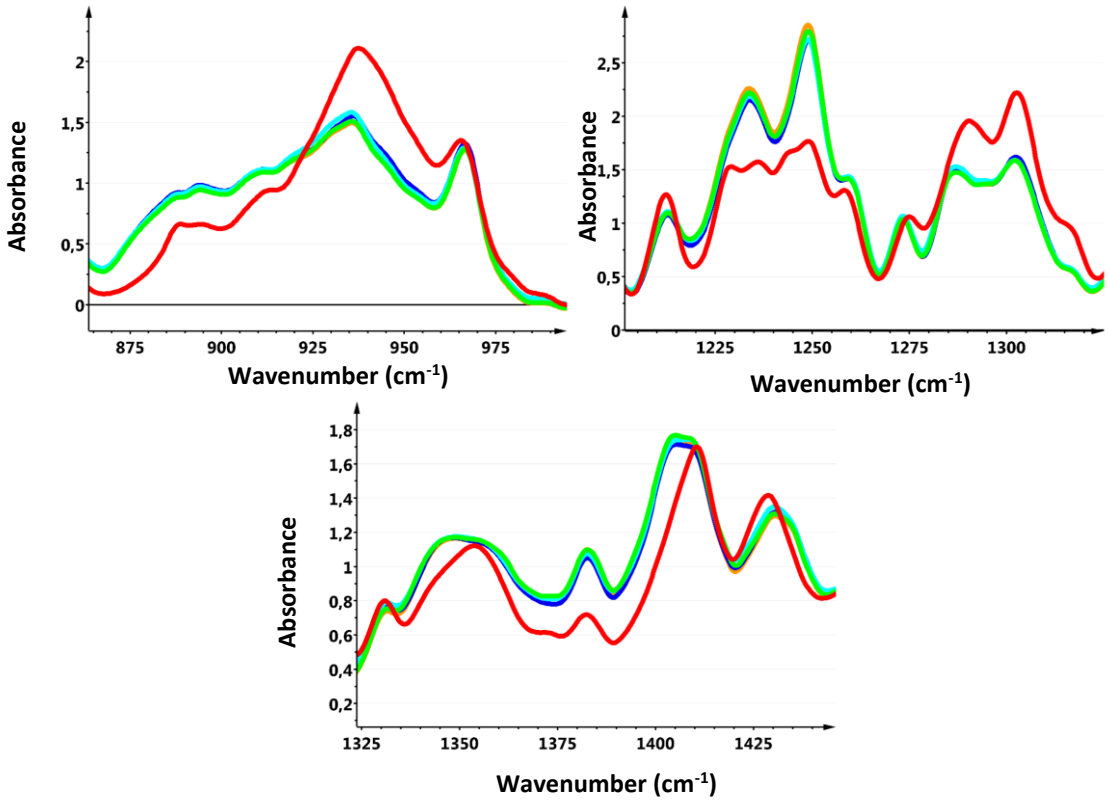

Fig. 4.23: FT-IR spectra of 30:20:50 MPT:MA:BA physical mixture (red), fresh extrudates (green), 1 week (dark blue), 1 month (orange) and 3 months (light blue) storage at 40 °C.

As previously mentioned (see 4.4.3.3), several changes occured in the FT-IR spectrum of 30:20:50 MPT:MA:BA extrudates compared to the physical mixture: changes in ratio of the peaks in the 875-975 cm^{-1} band, broadening of the peak in the 1390-1420 cm^{-1} and peak shifts to a lower wavenumber. All these spectral changes remained almost identical during 3 months storage at 25 °C and 40 °C, indicating that the intermolecular interactions were maintained during storage, as shown in Fig. 4.23.

4.5.1.4 MDSC

Table 4.5 illustrates the melting behaviour of the extrudates during storage at 25 °C and 40 °C. During storage, no clear trend in melting enthalpy could be observed. Therefore, stability testing after 6 months and 1 year is necessary. No significant changes in peak melting temperature of myristic acid and behenic acid were observed.

Table 4.5: Melting enthalpy and peak melting temperature of the 30:20:50 MPT:MA:BA extrudates immediately after manufacturing and after storage at 25 °C and 40 °C.

	Enthalpy (J/g)		Peak temperature (°C)	
	MA	**BA**	**MA**	**BA**
Fresh extrudates	43.3 ± 0.3	113.9 ± 0.7	42.8 ± 0.1	69.0 ± 0.1
1 week 25 °C	44.6 ± 0.3	114.5 ± 1.5	43.0 ± 0.2	69.0 ± 0.2
1 month 25 °C	45.7 ± 0.1	116.5 ± 1.3	43.2 ± 0.1	69.0 ± 0.2
3 months 25 °C	45.0 ± 0.2	112.6 ± 0.8	43.3 ± 0.1	69.1 ± 0.2
1 week 40 °C	45.2 ± 0.7	115.3 ± 0.5	43.3 ± 0.1	69.0 ± 0.1
1 month 40 °C	45.8 ± 0.3	114.6 ± 0.9	43.9 ± 0.1	69.1 ± 0.2
3 months 40 °C	46.5 ± 0.2	112.1 ± 0.4	44.3 ± 0.1	69.1 ± 0.2

4.5.1.5 X-ray diffraction

Fig. 4.24 shows the diffraction patterns of the 30:20:50 MPT:MA:BA extrudates immediately after extrusion and after 3 months storage at 25 °C and 40 °C. No significant differences could be observed between the X-ray patterns of the fresh and stored extrudates. These results confirm the results obtained using Raman spectroscopy and MDSC: the solid state of the extrudates had not changed after 3 months storage at 25 °C and 40 °C compared to the extrudates immediately after manufacturing.

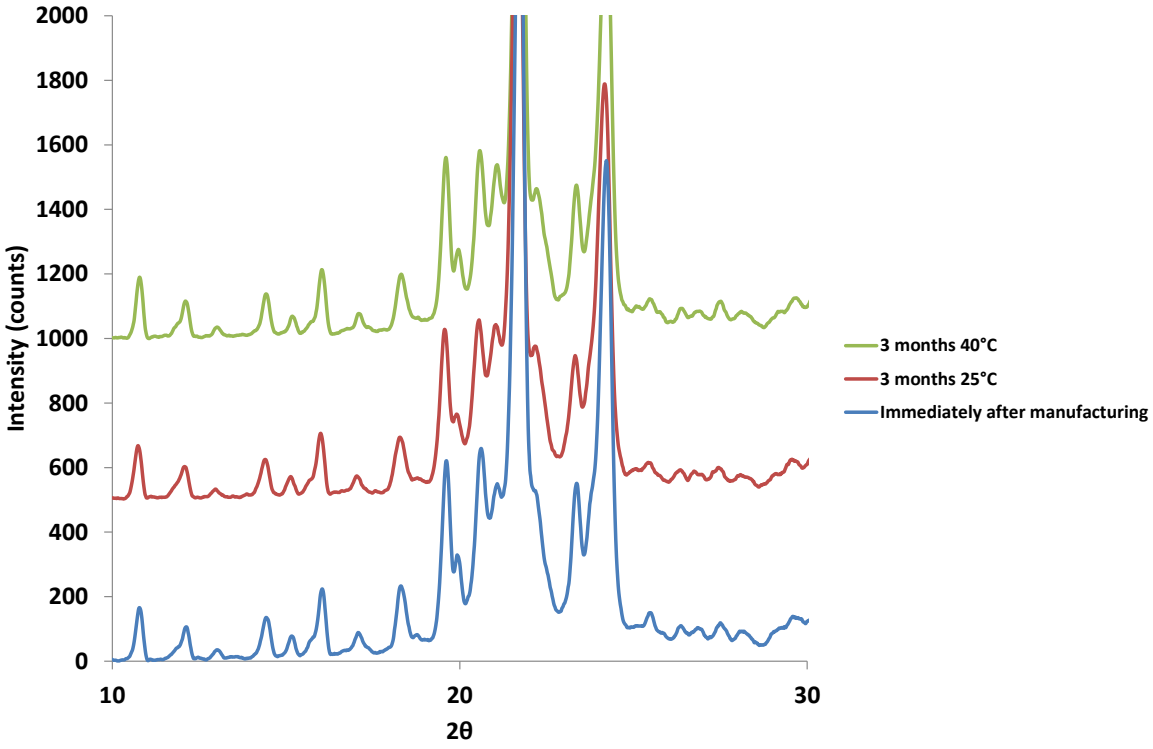

Figure 4.24: X-ray diffraction patterns of the 30:20:50 MPT:MA:BA fresh formulation (blue), after 3 months storage at 25 °C (red) and 40 °C (green).

4.5.1.6 Conclusion

Even though the in vitro drug release profile changed during storage, Raman and FT-IR spectroscopy, MDSC and X-ray diffraction did not offer an explanation for this phenomenon. Raman spectroscopy, MDSC and XRD suggested that the solid state was not altered during storage. FT-IR spectroscopy indicated that the molecular interactions which occurred during processing remained intact during storage.

4.5.2 Prills 30% MPT 20% MA 50% BA

4.5.2.1 In vitro drug release

The drug release rate of the stored prills (Fig. 4.25) tended to be increased compared to the freshly prepared prills, however this difference was not significant ($f_2 < 50$). Storage during 3 months at 25°C and 40 °C did not affect the in vitro drug release rate. However, the drug release should be tested after 6 months and 1 year as well.

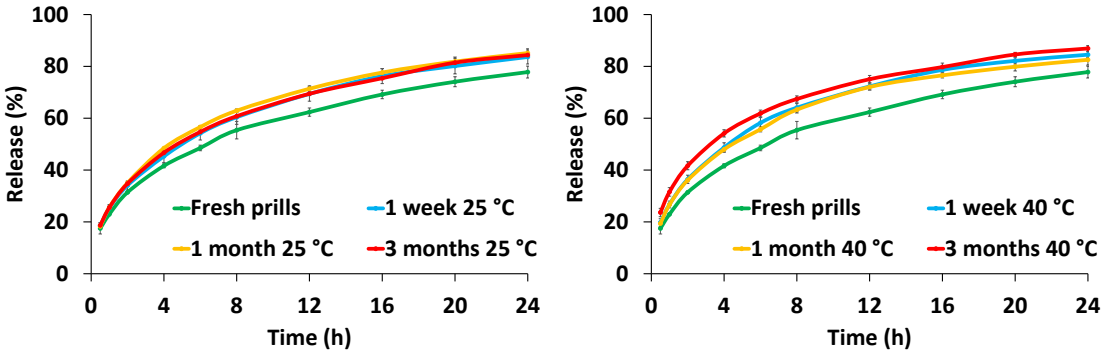

Figure 4.25: In vitro drug release of the 30:20:50 MPT:MA:BA prills immediately after extrusion (green), after 1 week (blue), 1 month (yellow) and 3 months (red) storage at 25 °C (left) and 40 °C (right).

4.5.2.2 Raman spectroscopy

Fig. 4.26 illustrates the Raman spectra of the prills immediately after manufacturing and after 1 week, 1 month and 3 months storage at 40 °C. In section 4.4.3.2, it was already mentioned that the fresh prills showed peak broadening in the 800-860 cm^{-1} and the 1070-1100 cm^{-1} bands, indicating loss in crystallinity of MPT and myristic acid. In the 920-980 cm^{-1} region, the intensity of the peaks had decreased significantly.

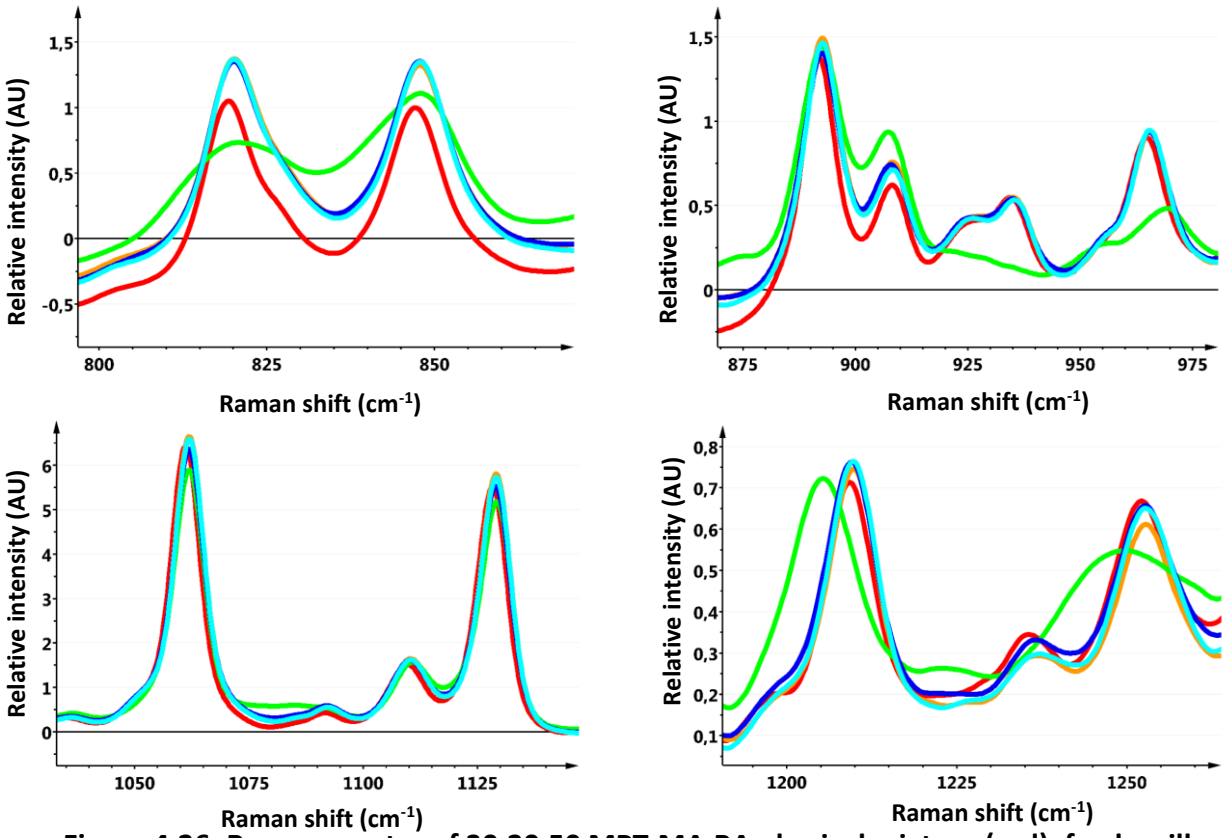

Figure 4.26: Raman spectra of 30:20:50 MPT:MA:BA physical mixture (red), fresh prills (green), 1 week (dark blue), 1 month (orange) and 3 months (light blue) storage at 40 °C.

However, after one week storage, the bands appeared sharper, indicating recrystallization of MPT and myristic acid. This change in solid state did not affect the in vitro drug release profile of the prills as seen in Fig. 4.23. After 1 month and 3 months storage, no further changes in the Raman spectra were observed. Identical observations were made for the prills stored at 25 °C (data not shown).

4.5.2.3 FT-IR analysis

Fig. 4.27 illustrates the FT-IR spectra of the prills immediately after manufacturing and after 1 week, 1 month and 3 months storage at 40 °C. The peak in the 800-850 cm^{-1} band had broadened in the spectra of the prills immediately after processing, indicating a decrease in crystallinity. After one week storage at 25 °C and 40 °C, the peak had sharpened again, suggesting recrystallization of MPT.

The fresh prills showed a change in ratio in the 1220-1320 cm^{-1} band compared to the physical mixture, indicating intermolecular interactions between MPT and the fatty acids. The change in ratio remained equal during storage, however, the peaks in the 1220-1260 cm^{-1} band appeared sharpened after storage compared with the fresh prills, therefore indicating recrystallization of the compounds.

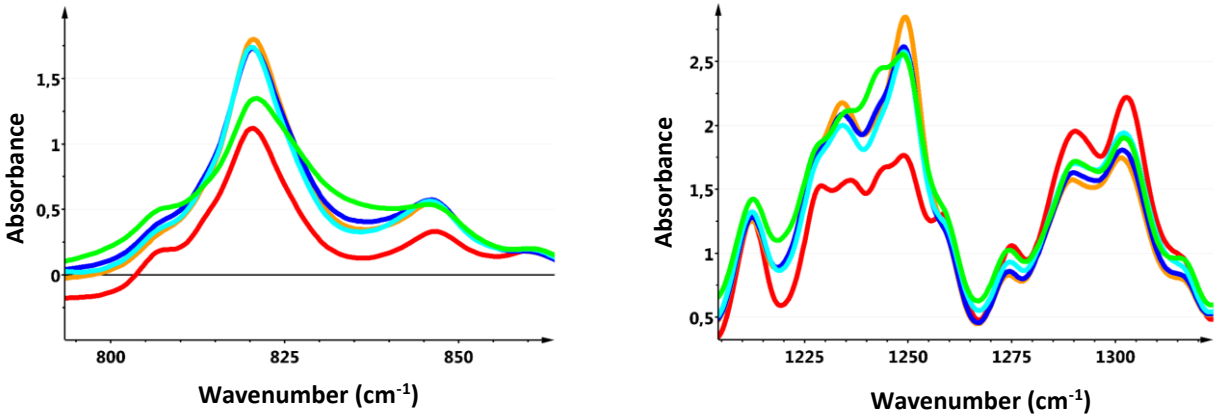

Fig. 4.27: FT-IR spectra of 30:20:50 MPT:MA:BA physical mixture (red), fresh prills (green), 1 week (dark blue), 1 month (orange) and 3 months (light blue) storage at 40 °C.

4.5.2.4 MDSC

Table 4.6 shows the melting enthalpy and peak melting temperature of 30:20:50 MPT:MA:BA prills, immediately after processing and during storage at 25 °C and 40 °C. After 1 week storage at both 25 °C and 40 °C, a higher melting enthalpy could be observed, indicating a higher degree of crystallinity. These results confirmed the Raman and FT-IR spectra: after one week of storage, MPT and myristic acid were more crystalline in comparison with the prills immediately after manufacturing. During storage, no clear trend in melting enthalpy could be observed. Therefore, stability tests after 6 months and 1 year are necessary. The peak melting temperature remained similar during storage.

Table 4.6 : Melting enthalpy and peak melting temperature of the 30:20:50 MPT:MA:BA prills immediately after manufacturing and after storage at 25 °C and 40 °C.

	Melting enthalpy (J/g)	Peak temperature (°C)
Fresh prills	137.7 ± 3.1	68.2 ± 0.1
1 week 25 °C	144.8 ± 2.4	68.3 ± 0.1
1 month 25 °C	147.6 ± 1.5	68.2 ± 0.1
3 months 25 °C	141.7 ± 4.2	68.4 ± 0.1
1 week 40 °C	148.1 ± 2.1	68.4 ± 0.2
1 month 40 °C	149.9 ± 1.7	68.7 ± 0.2
3 months 40 °C	145.2 ± 2.3	68.6 ± 0.1

4.5.2.5 X-ray diffraction

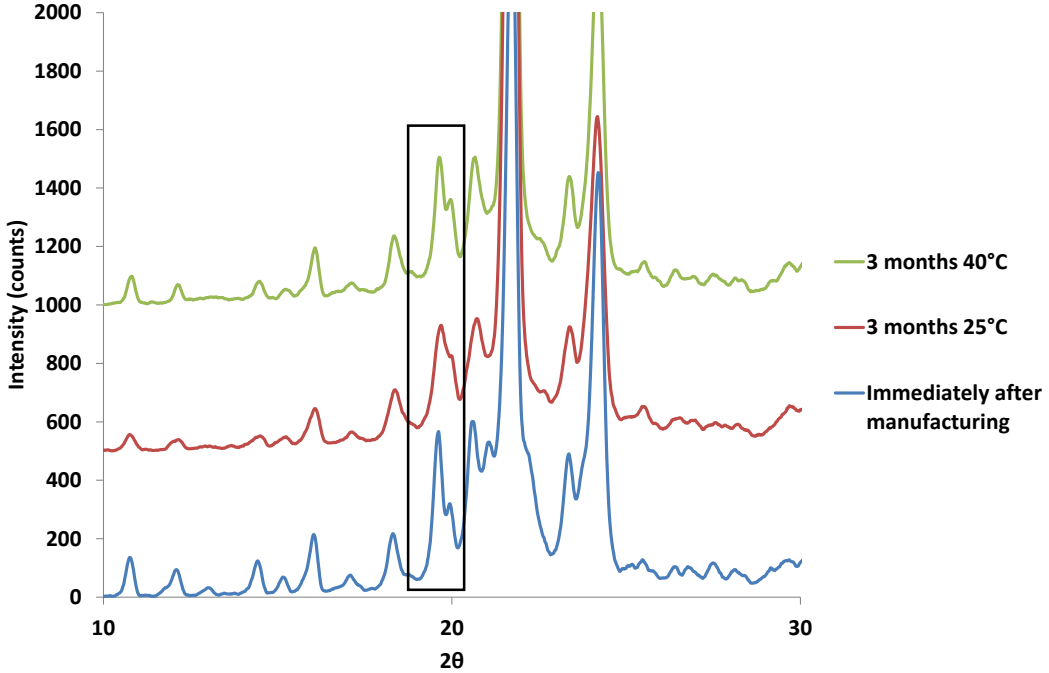

Fig. 4.28: X-ray patterns of the prills immediately after manufacturing (blue), after 3 months storage at 25 °C (red) and 40 °C (green).

Fig. 4.28 illustrates the X-ray diffraction patterns of the 30:20:50 MPT:MA:BA prills immediately after extrusion and after 3 months storage at 25 °C and 40 °C. The peak in the 18°-20° (2θ) region (attributed to mainly MPT) had broadened after 3 months storage in comparison with the fresh prills. This suggests a decrease in crystallinity during storage. The reason for this phenomenon is still unclear.

4.5.2.6 Conclusion

The in vitro release rate of the 30:20:50 MPT:MA:BA prills did not change during storage. The Raman spectra of the prills immediately after processing showed a lower degree of crystallinity of MPT and myristic acid compared to the physical mixture. After 1 week storage at 25 °C and 40 °C, the peaks had sharpened again, indicating recrystallization of the compounds. After 1 month and 3 months storage, no further changes in solid state were observed. FT-IR spectroscopy and MDSC confirmed these results.

4.5.3 Extrudates 30% MPT 70% BA

4.5.3.1 In vitro drug release

Fig. 4.29 shows the MPT release from the extrudates containing 30% MPT and 70% behenic acid. The release rate remained stable during 3 months storage at 25 °C and 40 °C.

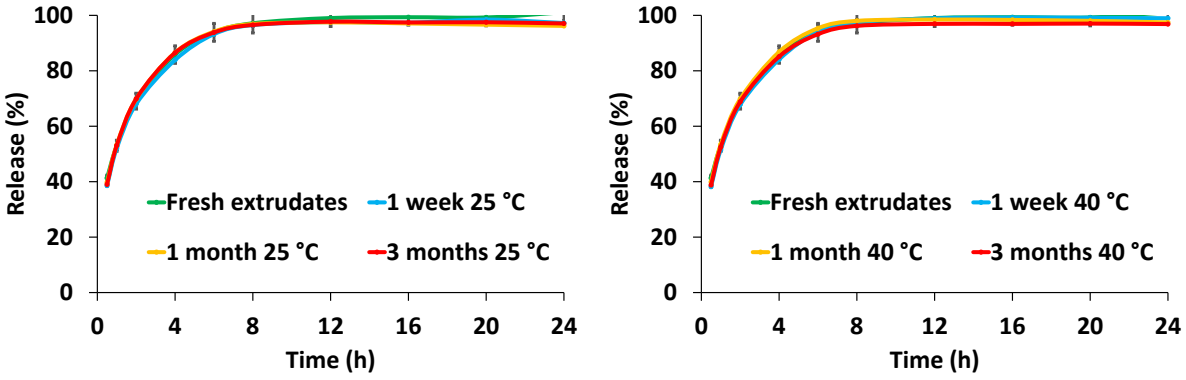

Figure 4.29: In vitro drug release of the 30:70 MPT:BA extrudates immediately after extrusion (green), after 1 week (blue), 1 month (yellow) and 3 months (red) storage at 25 °C (left) and 40 °C (right).

4.5.3.2 Raman spectroscopy

The Raman spectra of the fresh extrudates and after 1 week, 1 month and 3 months storage at 25 °C and 40 °C were similar (data not shown), indicating that the crystalline structure of the fatty acids and MPT was maintained during storage.

4.5.3.3 FT-IR analysis

The FT-IR spectra of the fresh extrudates revealed a changed ratio in the 1220-1260 cm^{-1} band compared to the physical mixture. These differences were similar in the spectra of the extrudates stored at 25 °C (data not shown) and 40 °C (Fig. 4.30) after 1 week, 1 month and 3 months of storage.

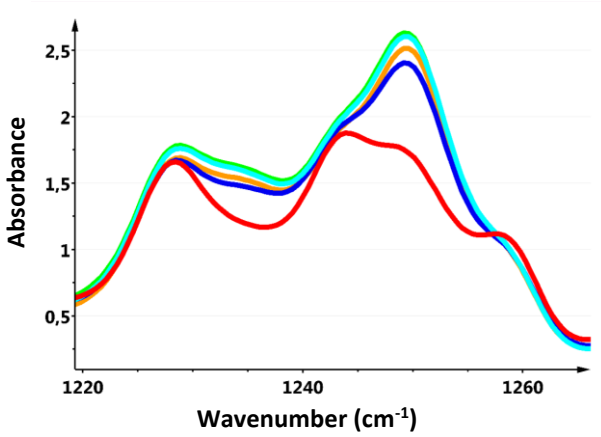

Figure 4.30: FT-IR spectra of physical mixture (red), fresh extrudates (green), 1 week (dark blue), 1 month (orange) and 3 months (light blue) storage at 40 °C.

4.5.3.4 MDSC

Table 4.7 shows the melting enthalpy, the melt onset and the peak melting temperature of the 30:70 MPT:BA extrudates immediately after manufacturing and after storage at 25 °C and 40 °C. During storage at 25 °C and 40 °C, only minimal fluctuations in onset melting temperature and peak melting temperature were observed. The melting endotherms of the fresh and stored extrudates had a similar shape (data not shown).

Table 4.7: Melting enthalpy, melt onset and peak melting temperature of 30:70 MPT:BA extrudates immediately after manufacturing and after storage at 25 °C and 40 °C.

	Enthalpy (J/g)	Onset temperature (°C)	Peak temperature (°C)
Fresh extrudates	183.7 ± 2.6	72.3 ± 0.1	74.8 ± 0.1
1 week 25 °C	182.6 ± 2.0	72.1 ± 0.1	74.7 ± 0.1
1 month 25 °C	182.6 ± 4.6	72.3 ± 0.1	74.8 ± 0.1
3 months 25 °C	179.5 ± 1.0	72.3 ± 0.1	74.9 ± 0.2
1 week 40 °C	182.9 ± 1.6	72.2 ± 0.1	74.7 ± 0.1
1 month 40 °C	180.5 ± 0.5	72.4 ± 0.2	74.8 ± 0.1
3 months 40 °C	177.8 ± 2.4	72.3 ± 0.1	75.0 ± 0.1

4.5.3.5 X-ray diffraction

Fig. 4.31 represents the diffraction patterns of the 30:70 MPT:BA physical mixture, the corresponding extrudates and the extrudates after 3 months storage at 25 °C and 40 °C. No significant differences could be detected between storage at 25 °C and 40 °C, indicating that the solid state of the extrudates was not changed during storage and therefore confirming the results obtained by MDSC and Raman spectroscopy.

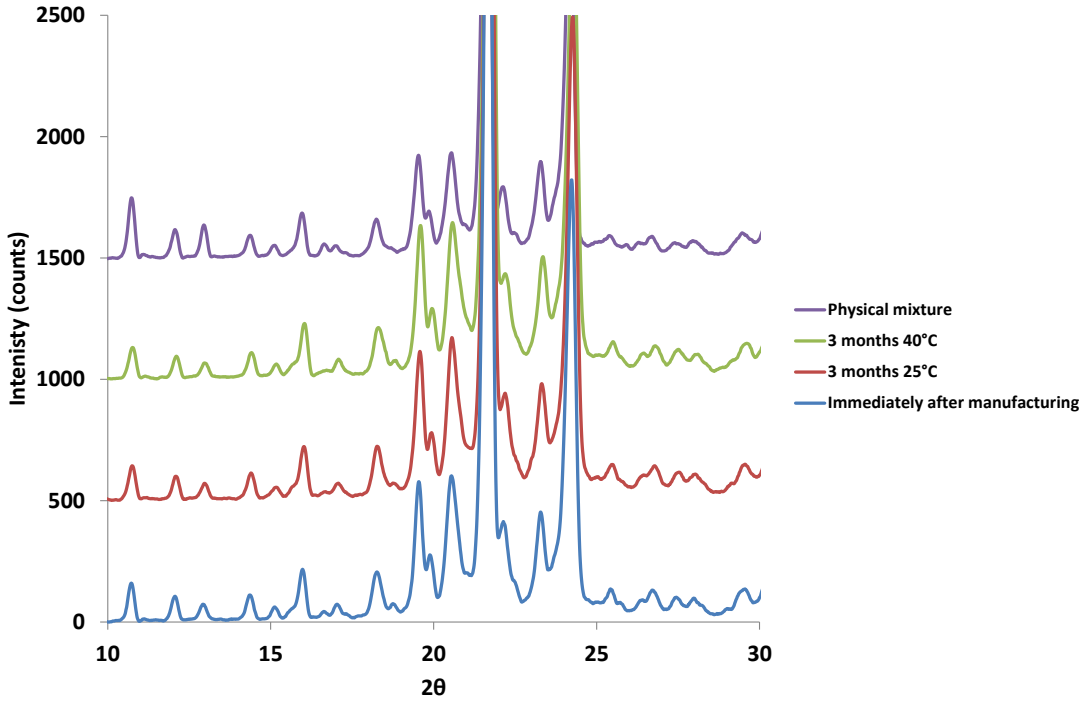

Figure 4.31: X-ray patterns of the physical mixture 30:70 MPT:BA (purple), the fresh extrudates (blue) and the extrudates after 3 months storage at 25 °C (red) and 40 °C (green).

4.5.3.6 Conclusion

No changes in drug release rate from 30:70 MPT:BA extrudates could be observed during storage. Raman spectroscopy, MDSC and XRD suggested that the solid state of the extrudates did not change during storage.

5 CONCLUSION

Controlled release formulations were successfully produced via both extrusion and prilling by adding a certain percentage of myristic acid to the behenic acid matrix. The in vitro dissolution rate of the 30:70 MPT:BA extrudates was significantly faster compared to the 30:20:50 MPT:MA:BA extrudates and prills. As myristic acid is less hydrophobic than behenic acid, these results were not expected. The difference could be explained by molecular interactions between the fatty acids and/or between MPT and the fatty acids.

In the Raman spectra of 2:5 MA:BA extrudates, an additional peak appeared at 859 cm^{-1}. As it did not appear in spectra of extrudates and prills of the pure compounds, it could probably be attributed to intermolecular interactions between both fatty acids during extrusion. The peak was also present in spectra of the 30:20:50 MPT:MA:BA extrudates, but not in the corresponding prills, suggesting more interactions occurred during extrusion caused by more intense mixing by the screws. The FT-IR results confirmed this assumption.

Peak broadening in the Raman spectra of the 30:20:50 MPT:MA:BA prills immediately after manufacturing compared to the physical mixture indicated a decrease in crystallinity of myristic acid and the presence of amorphous MPT. During storage at 25 °C and 40 °C, the peaks had sharpened again, indicating recrystallization during storage. However, no significant differences in drug release rate were observed during storage.

The drug release rate from 30:20:50 MPT:MA:BA extrudates was significantly decreased after 1 month and 3 months storage at 40 °C compared to immediately after processing. The reason for this phenomenon is still unclear, as Raman and FT-IR spectroscopy, MDSC and XRD revealed no changes during storage. Storage at 25 °C during 3 months did not affect the in vitro release of MPT.

6 REFERENCES

1. Crowley MM, Zhang F, Repka MA, Thumma S, Upadhye SB, Battu SK, et al. Pharmaceutical applications of hot-melt extrusion: Part I. Drug Dev Ind Pharm. 2007;33(9):909-26.

2. Lang B, McGinity JW, Williams RO, 3rd. Hot-melt extrusion--basic principles and pharmaceutical applications. Drug Dev Ind Pharm. 2014;40(9):1133-55.

3. Repka MA, Battu SK, Upadhye SB, Thumma S, Crowley MM, Zhang F, et al. Pharmaceutical applications of hot-melt extrusion: Part II. Drug Dev Ind Pharm. 2007;33(10):1043-57.

4. De Brabander C, Vervaet C, Remon JP. Development and evaluation of sustained release mini-matrices prepared via hot melt extrusion. J Control Release. 2003;89(2):235-47.

5. Vithani K, Maniruzzaman M, Slipper IJ, Mostafa S, Miolane C, Cuppok Y, et al. Sustained release solid lipid matrices processed by hot-melt extrusion (HME). Colloid Surface B. 2013;110:403-10.

6. Zhang F, McGinity JW. Properties of sustained-release tablets prepared by hot-melt extrusion. Pharm Dev Technol. 1999;4(2):241-50.

7. Maniruzzaman M, Boateng JS, Bonnefille M, Aranyos A, Mitchell JC, Douroumis D. Taste masking of paracetamol by hot-melt extrusion: An in vitro and in vivo evaluation. Eur J Pharm Biopharm. 2012;80(2):433-42.

8. Maniruzzaman M, Boateng JS, Chowdhry BZ, Snowden MJ, Douroumis D. A review on the taste masking of bitter APIs: hot-melt extrusion (HME) evaluation. Drug Dev Ind Pharm. 2014;40(2):145-56.

9. Witzleb R, Kanikanti VR, Hamann HJ, Kleinebudde P. Solid lipid extrusion with small die diameters - Electrostatic charging, taste masking and continuous production. Eur J Pharm Biopharm. 2011;77(1):170-7.

10. Kleinebudde P. Pharmaceutical Product Design: Tailored Dissolution of Drugs by Different Extrusion Techniques. Chem-Ing-Tech. 2011;83(5):589-97.

11. Hot melt extrusion - Continuous quality [02/11/2014]. Available from: http://www.industry.siemens.com/topics/global/en/magazines/process-news/pharmaceutical/pages/hot-melt-extrusion.aspx.

12. Trivedi NR, Rajan MG, Johnson JR, Shukla AJ. Pharmaceutical approaches to preparing pelletized dosage forms using the extrusion-spheronization process. Critical reviews in therapeutic drug carrier systems. 2007;24(1):1-40.

13. Breitenbach J. Melt extrusion: from process to drug delivery technology. Eur J Pharm Biopharm. 2002;54(2):107-17.

14. Saerens L, Dierickx L, Lenain B, Vervaet C, Remon JP, De Beer T. Raman spectroscopy for the in-line polymer-drug quantification and solid state characterization during a pharmaceutical hot-melt extrusion process. Eur J Pharm Biopharm. 2011;77(1):158-63.

15. Saerens L, Vervaet C, Remon JP, De Beer T. Visualization and Process Understanding of Material Behavior in the Extrusion Barrel during a Hot-Melt Extrusion Process Using Raman Spectroscopy. Anal Chem. 2013;85(11):5420-9.

16. Saerens L, Vervaet C, Remon JP, De Beer T. Process monitoring and visualization solutions for hot-melt extrusion: a review. Journal of Pharmacy and Pharmacology. 2014;66(2):180-203.

17. Martin C. Twin Screw Extrusion for Pharmaceutical Processes. In: Repka MA, Langley N, DiNunzio J, editors. Melt Extrusion. AAPS Advances in the Pharmaceutical Sciences Series2013. p. 474.

18. Del Gaudio P, Russo P, Rosaria Lauro M, Colombo P, Aquino RP. Encapsulation of ketoprofen and ketoprofen lysinate by prilling for controlled drug release. Aaps Pharmscitech. 2009;10(4):1178-85.

19. Yuan W, Chuanping B, Yuxin Z. An innovated tower-fluidized bed prilling process. Chinese J Chem Eng. 2007;15(3):424-8.

20. Pivette P, Faivre V, Daste G, Ollivon M, Lesieur S. Rapid cooling of lipid in a prilling tower. J Therm Anal Calorim. 2009;98(1):47-55.

21. Vervaeck A, Monteyne T, Saerens L, De Beer T, Remon JP, Vervaet C. Prilling as manufacturing technique for multiparticulate lipid/PEG fixed-dose combinations. European journal of pharmaceutics and biopharmaceutics : official journal of Arbeitsgemeinschaft fur Pharmazeutische Verfahrenstechnik eV. 2014.

22. Vervaeck A, Saerens L, De Geest BG, De Beer T, Carleer R, Adriaensens P, et al. Prilling of fatty acids as a continuous process for the development of controlled release multiparticulate dosage forms. Eur J Pharm Biopharm. 2013;85(3):587-96.

23. New Chronosphere formulation offers significant advantages for people with epilepsy [07/12/2014]. Available from: http://news.cision.com/no/sanofi-aventis-norge-as/r/new-chronosphere--formulation-offers-significant-advantages-for-people-with-epilepsy,c105669.

24. Shukla D, Chakraborty S, Singh S, Mishra B. Pastillation: A novel technology for development of oral lipid based multiparticulate controlled release formulation. Powder Technol. 2011;209(1-3):65-72.

25. Sequier F, Faivre V, Daste G, Renouard M, Lesieur S. Critical parameters involved in producing microspheres by prilling of molten lipids: from theoretical prediction of particle size to practice. European journal of pharmaceutics and biopharmaceutics : official journal of Arbeitsgemeinschaft fur Pharmazeutische Verfahrenstechnik eV. 2014;87(3):530-40.

26. Rosiaux Y, Jannin V, Hughes S, Marchaud D. Solid lipid excipients - Matrix agents for sustained drug delivery. J Control Release. 2014;188:18-30.

27. Reitz C, Kleinebudde P. Solid lipid extrusion of sustained release dosage forms. Eur J Pharm Biopharm. 2007;67(2):440-8.

28. Vaassen J, Bartscher K, Breitkreutz J. Taste masked lipid pellets with enhanced release of hydrophobic active ingredient. Int J Pharm. 2012;429(1-2):99-103.

29. Krause J, Thommes M, Breitkreutz J. Immediate release pellets with lipid binders obtained by solvent-free cold extrusion. Eur J Pharm Biopharm. 2009;71(1):138-44.

30. Pivette P, Faivre V, Mancini L, Gueutin C, Daste G, Ollivon M, et al. Controlled release of a highly hydrophilic API from lipid microspheres obtained by prilling: analysis of drug and water diffusion processes with X-ray-based methods. J Control Release. 2012;158(3):393-402.

31. Yan X, He H, Meng J, Zhang C, Hong M, Tang X. Preparation of lipid aspirin sustained-release pellets by solvent-free extrusion/spheronization and an investigation of their stability. Drug Dev Ind Pharm. 2012;38(10):1221-9.

32. Windbergs M, Gueres S, Strachan CJ, Kleinebudde P. Two-Step Solid Lipid Extrusion as a Process to Modify Dissolution Behavior. Aaps Pharmscitech. 2010;11(1):2-8.

33. Michalk A, Kanikanti VR, Hamann HJ, Kleinebudde P. Controlled release of active as a consequence of the die diameter in solid lipid extrusion. J Control Release. 2008;132(1):35-41.

34. Faisal W, Ruane-O'Hora T, O'Driscoll CM, Griffin BT. A novel lipid-based solid dispersion for enhancing oral bioavailability of Lycopene - In vivo evaluation using a pig model. Int J Pharmaceut. 2013;453(2):307-14.

35. Chauhan B, Shimpi S, Mahadik KR, Paradkar A. Preparation and evaluation of floating risedronate sodium-Gelucire 43/01 formulations. Drug Dev Ind Pharm. 2005;31(9):851-60.

36. Windbergs M, Strachan CJN, Kleinebudde P. Influence of structural variations on drug release from lipid/polyethylene glycol matrices. Eur J Pharm Sci. 2009;37(5):555-62.

37. Windbergs M, Strachan CJ, Kleinebudde P. Understanding the solid-state behaviour of triglyceride solid lipid extrudates and its influence on dissolution. Eur J Pharm Biopharm. 2009;71(1):80-7.

38. Sutananta W, Craig DQM, Newton JM. The Effects of Aging on the Thermal-Behavior and Mechanical-Properties of Pharmaceutical Glycerides. Int J Pharmaceut. 1994;111(1):51-62.

39. Controlled Drug Delivery [03/11/2014]. Available from: http://dc339.4shared.com/doc/hoNfFV6S/preview.html.

40. Tran PHL, Tran TTD, Park JB, Lee BJ. Controlled Release Systems Containing Solid Dispersions: Strategies and Mechanisms. Pharmaceutical research. 2011;28(10):2353-78.

41. Lijst van de geneesmiddelen met nauwe therapeutisch-toxische marge [03/11/2014]. Available from: http://www.bcfi.be/folia/index.cfm?FoliaWelk=F41N07E

42. Ummadi S, Shravani B, Raghavendra Rao NG, Srikanth Reddy M, Sanjeev Nayak B. Overview on Controlled Release Dosage Form. International Journal of Pharma Sciences. 2013;3(4):258-69.

43. Janssens S, Van den Mooter G. Review: physical chemistry of solid dispersions. The Journal of pharmacy and pharmacology. 2009;61(12):1571-86.

44. Leuner C, Dressman J. Improving drug solubility for oral delivery using solid dispersions. European journal of pharmaceutics and biopharmaceutics : official journal of Arbeitsgemeinschaft fur Pharmazeutische Verfahrenstechnik eV. 2000;50(1):47-60.

45. Dhirendra K, Lewis S, Udupa N, Atin K. Solid Dispersions: A Review. Pakistan journal of pharmaceutical sciences. 2009;22(2):234-46.

46. Chiou WL, Riegelman S. Pharmaceutical applications of solid dispersion systems. J Pharm Sci. 1971;60(9):1281-302.

47. Vasconcelos T, Sarmento B, Costa P. Solid dispersions as strategy to improve oral bioavailability of poor water soluble drugs. Drug Discov Today. 2007;12(23-24):1068-75.

48. Dey NS, Majumadar S, Rao MEB. Multiparticulate Drug Delivery Systems for Controlled Release. Trop J Pharm Res. 2008;7(3):1067-75.

49. Roy P, Shahiwala A. Multiparticulate formulation approach to pulsatile drug delivery: Current perspectives. J Control Release. 2009;134(2):74-80.

50. Newton JM. Gastric emptying of multi-particulate dosage forms. Int J Pharmaceut. 2010;395(1-2):2-8.

51. Beta-blokkers [11/10/2014]. Available from: http://www.bcfi.be/GGR/Index.cfm?ggrWelk=/nIndex/GGR/Stof/IN_M.cfm.

52. Merck Index, fifteenth edition.

53. Metoprolol [01/12/2014]. Available from: http://pubchem.ncbi.nlm.nih.gov/compound/4171?from=summary#section=Other-Experimental-Properties.

54. Reddy BBK, Karunakar A. Biopharmaceutics Classification System: A Regulatory Approach. Dissolut Technol. 2011;18(1):31-7.

55. Lopressor (metoprolol tartrate) [11/10/2014]. Available from: http://www.rxlist.com/lopressor-drug.htm.

56. Behenic acid [11/10/2014]. Available from: pubchem.nobi.nlm.nih.gov/rest/chemical/behenic+acid.

57. Behenic acid - structural formula [11/10/2014]. Available from: http://commons.wikimedia.org/wiki/File:Behenic_acid.svg.

58. Myristic acid [11/10/2014]. Available from: http://pubchem.ncbi.nlm.nih.gov/rest/chemical/myristic+acid#x27.

59. Myristic acid - structural formula [11/10/2014]. Available from: http://commons.wikimedia.org/wiki/File:Myristic_acid.svg.

60. Malfroot P. Extrusie en prilling van vetzuren voor de ontwikkeling van multiparticulaire doseervormen met gecontroleerde vrijstelling 2014.

61. Shah VP, Tsong Y, Sathe P, Liu JP. In vitro dissolution profile comparison - Statistics and analysis of the similarity factor, f(2). Pharmaceutical research. 1998;15(6):889-96.

62. Bright A, Renuga Devi S, Gunasekaran S. Spectroscopical vibrational band assignment and qualitative analysis of biomedical compounds with cardiovascular activity. International Journal of ChemTech Research. 2010;2(1):379-88.

63. De Gelder J, De Gussem K, Vandenabeele P, Moens L. Reference database of Raman spectra of biological molecules. J Raman Spectrosc. 2007;38(9):1133-47.

64. Smith B. Infrared spectral interpretation - A systematic approach1998.

65. Windbergs M, Strachan CJ, Kleinebudde P. Influence of the composition of glycerides on the solid-state behaviour and the dissolution profiles of solid lipid extrudates. Int J Pharmaceut. 2009;381(2):184-91.

66. Yongcheng L, Huishi P, Zhefei G, Ling L, Yixuan D, Ge L, et al. Interactions between drugs and polymers influencing hot melt extrusion. Journal of Pharmacy And Pharmacology. 2013;66(2):148-66.